Morphological Change of a Developed Barrier Island due to Hurricane Forcing

Stephanie Marie Smallegan

Dissertation submitted to the Faculty of the
Virginia Polytechnic Institute and State University
in partial fulfillment of the requirements for the degree of

Doctor of Philosophy
in
Civil Engineering

Jennifer L. Irish, Chair
Christopher J. Roy
Nina Stark
Ap R. Van Dongeren
Robert Weiss

March 15, 2016
Blacksburg, Virginia

Keywords: Hurricane Sandy, Barrier Island, Breach, Overwash, Seawall

Morphological Change of a Developed Barrier Island due to Hurricane Forcing

Stephanie Marie Smallegan

ABSTRACT

An estimated 10% of the world's population lives in low-lying coastal regions, which are vulnerable to storm surge and waves capable of causing loss of lives and billions of dollars in damage to coastal infrastructure. Among the most vulnerable coastlines are barrier islands, which often act as the first line of defense against storms for the mainland coast. In this dissertation, the physical damage to a developed barrier island (Bay Head, NJ, USA) caused by erosion during Hurricane Sandy (2012) is evaluated using the numerical model, XBeach. Three main objectives of this work are to evaluate the wave-force reducing capabilities of a buried seawall, the effects of bay surge on morphological change and the effectiveness of adaptation strategies to rising sea levels. According to simulation results, a buried seawall located beneath the nourished dunes in Bay Head reduced wave attack by a factor of 1.7 compared to locations without a seawall. The structure also prevented major erosion by blocking bay surge from inundating dunes from the backside, as observed in locations not fronted with a seawall. Altering the timing and magnitude of bay storm surge, the buried seawall continued to protect the island from catastrophic erosion under all conditions except for a substantial increase in bay surge. However, in the absence of a seawall, the morphological response was highly dependent on bay surge levels with respect to ocean side surge. Compared to the damage sustained by the island during Hurricane Sandy, greater erosion was observed on the island for an increase in bay surge magnitude or when peak bay surge occurred after peak ocean surge. Considering sea level rise, which affects bay and ocean surge levels, adaptation strategies were evaluated on the protection afforded to the dune system and backbarrier. Of the sea level rise scenarios and adaptation strategies considered, raising the dune and beach protected the island under moderate rises in sea level, but exacerbated backbarrier erosion for the most extreme scenario. Although an extreme strategy, raising the island is the only option considered that protected the island from catastrophic erosion under low, moderate and extreme sea level rise.

This material is based upon work supported by the National Oceanic and Atmospheric Administration, U.S. Department of Commerce, via award number NA14OAR4170093 to Virginia Sea Grant; the National Science Foundation Graduate Research Fellowship Program via grant number DGE-1148903; and National Science Foundation via grant number EAR-1312813.

Acknowledgments

My sincerest gratitude goes to my advisor, Dr. Jennifer Irish, for her support, encouragement and guidance throughout the years. I have become an independent researcher, a better author, and a confident instructor because of her leadership. She was flexible when, after Hurricane Sandy made landfall, I decided to switch the focus of my dissertation work from long-term shoreline change to erosion on barrier islands. Dr. Irish has allowed me the freedom to pursue my own academic career, earn additional graduate certificates, teach my own Fluid Mechanics class, and apply for my own funding. She also encouraged me to apply for my current position at the University of South Alabama. Thank you, Dr. Irish, for helping me grow into the researcher and academic I am today.

I also want to thank my committee members Dr. Chris Roy, Dr. Nina Stark, Dr. Ap Van Dongeren, and Dr. Robert Weiss for your suggestions, questions, and support on my dissertation work. I am honored to have learned from and worked with each of you, and hope to continue to collaborate in the future.

To Kyle, my heart and soul - I thank him for giving up a career he loved to move to Virginia with me, changing life paths completely, starting a career, moving with me again... it has been a roller coaster ride! He has always been supportive and encouraging. I am incredibly excited to finally be able to settle into our careers, create a home together and enjoy the rest of our lives.

Lastly, I thank my family, particularly for my prayin' mama and daddy. Those prayers held me together many days, and so did their phone calls, texts, and random funnies. Thank you, my God, for hearing those prayers. I am humbled and beyond blessed to have had this experience.

Contents

List of Figures

List of Tables

ATTRIBUTION

In this manuscript-based dissertation, co-authors and affiliations are listed at the beginning of each chapter. Their contributions are as follows. Jennifer Irish, as primary advisor of this work, guided its progress and made suggestions for model simulations and result analyses. Irish edited all manuscripts and instructed me on writing and submitting peer-reviewed manuscripts. Ap Van Dongeren helped me develop my understanding of XBeach and how the model calculates morphological change from its wave and flow modules. Van Dongeren made suggestions to increase model performance and speed of simulations and edited manuscripts for which he is a co-author. Joost Den Bieman taught me to use XBeach effectively and create model inputs, particularly the model grid, which is used throughout this disseration. Den Bieman also edited manuscripts for which he is a co-author.

Chapter 1

Introduction

Most of the world's coastlines consist of sandy beaches (Sorensen, 2005). Although beaches have different sediment compositions and are subject to varying wind and wave climates, they respond similarly to forcing mechanisms (Dean and Dalrymple, 2004). These processes include nearshore hydrodynamics, such as waves, currents, tides and storm surge; wind forcing, which builds and reshapes dunes via aeolian sediment transport; and human interaction, including infrastructure development, shoreline stabilization, beach nourishment or offshore installations. Sandy beaches and dunes respond to forcing mechanisms by absorbing energy while deforming, often resulting in significant erosion but also significant reductions in damage to inland regions. Morphological change can occur over hours or days (e.g. in response to storm forcing) or over decades to centuries (e.g. in response to sea level rise (SLR)).

Although sandy beaches are dynamic and continually impacted by coastal processes, they are important for sustaining local and global economies from ports, harbors, recreation and tourism, which attracts people to these areas (Dean and Dalrymple, 2004). Globally, 10% of the population reside in low-lying coastal regions, which are defined as having elevations less than 10 m above sea level (McGranahan et al., 2007). These regions account for only 2% of the world's land area and are particularly vulnerable to the coastal processes previously described (McGranahan et al., 2007). In the U.S., 52% of the population lives in coastal watershed counties (Crossett et al., 2013) and 3% live in regions affected by the 1% annual chance (100 yr) flood (Crowell et al., 2010). The economic cost of coastal disasters accounts for over half of the total damage due to all natural disasters combined, and these costs continue to increase as infrastructure is continually being built (Crossett et al., 2013; National Research Council, 2014; Smith and Katz, 2013). Therefore, millions of people and infrastructure worth billions of dollars (USD) are impacted by coastal processes, and a better understanding of these processes is necessary to prepare communities for impacts from coastal disasters.

Among the most vulnerable coastal regions are barrier islands, which make up 6.5% of the world's open ocean coastlines (Stutz and Pilkey, 2001). Barrier islands are often the first

line of defense against storms for the mainland coast, attenuating wave energy and serving as a barrier to storm surge (National Research Council, 2014). The vulnerability of barrier islands to storm surge and waves depends on several factors, including dune height, beach width, island width, topographic longshore variability and offshore bathymetric features (Claudino-Sales et al., 2008; Houser et al., 2008; Morton, 2002; Sallenger, 2000). In general, vulnerability increases as the volume of sediment available for transport decreases (Thieler and Young, 1991).

Sallenger (2000) categorizes the level of storm impact on barrier islands as regimes (Figure 1.1). The swash regime is the period during which storm impacts affect only the foreshore, and eroded sediment remains within the system to re-establish the dune. As storm impacts become more severe, the collision regime is reached. In this case, the berm and base of the dune are eroded and sediment is transported offshore such that it is not available for dune rebuilding. Next, the overwash regime is reached when dune crests are overtopped and sediment is transported landward from its originating dune. Lastly, the inundation regime refers to submergence of the island, which causes severe erosion and often the formation of a breach or new inlet through the barrier. These four impact regimes are used throughout this dissertation to refer to the severity of storm impact on barrier islands.

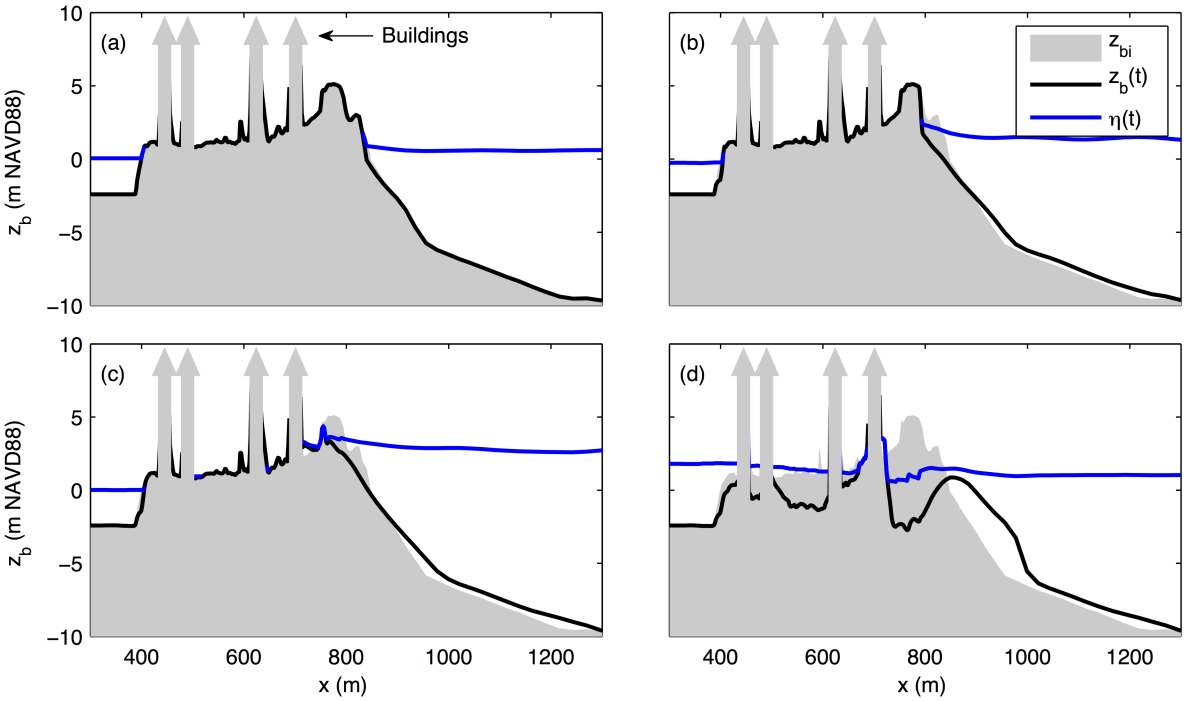

Figure 1.1: Impact regimes as defined by Sallenger (2000) of a developed barrier island profile (buildings are peaks in data): (a) swash regime, (b) collision regime, (c) overwash regime and (d) inundation regime. Initial island profile, z_{bi} (gray shaded) is shown for reference with time-varying cross-shore profile, $z_b(t)$ (black) and water level, $\eta(t)$ (blue).

To fortify sandy barrier islands against coastal processes, nature-based strategies, hard structures and combinations of these two designs have been implemented. In the U.S., the most common coastal risk reduction strategy is beach nourishment, a nature-based strategy intended to attenuate storm surge by allowing the beach and dune to deform (National Research Council, 2014). However, this mobilized sediment impacts local ecosystems and leads to subsequent re-nourishment projects (Cunniff and Schwartz, 2015). Hard structures, such as seawalls or revetments, are effective at reducing storm surge and wave impacts (Irish et al., 2013; Pilkey and Wright III, 1988); however, erosion on the seaward side of the seawall is often increased since seawalls reflect wave energy (Kraus and McDougal, 1996; National Research Council, 2014). Therefore, combining nature-based strategies with hard structures, such as an armored dune, has become an attractive option because adverse impacts are minimized while the benefits of each strategy are maintained. Due to the relatively rare occurrence of storms, the effectiveness of this type of coastal risk reduction strategy has been quantitatively assessed by few studies (Basco, 1998; Irish et al., 2013).

Although storm impacts on sandy beaches are typically governed by ocean surge and waves, barrier islands are also affected by hydrodynamics within the bay. Wind can increase bay surge levels and lead to inundation of the backbarrier region, which usually has the lowest elevations on the island (Kraus and Wamsley, 2003). Under extreme surge levels, the island may become completely submerged. In this case, the water level gradient between ocean and bay surge governs sediment deposition patterns (i.e. sediment is deposited seaward when the water level gradient is seaward sloping (Sherwood et al., 2014)). Since seaward-deposited sediment is quickly reworked by waves and tides, it is difficult to obtain accurate field measurements of deposit volumes; therefore, numerical models aid in determining the directionality of sediment transport and morphological change of the barrier island in response to storm forcing (Sherwood et al., 2014).

In addition to analyzing the effects of bay hydrodynamics on morphological change, numerical models can be used to estimate the future behavior of barrier islands as sea levels rise. Natural systems migrate landward via storm overwash (Gutierrez et al., 2007); however, on developed barrier islands, this landward movement is often prevented in order to protect infrastructure using nature-based and hard structures (Pilkey and Wright III, 1988). It is important to determine effective adaptation strategies to rising sea levels for the sustainability of barrier island systems.

The work presented in this dissertation aims to analyze the behavior of a narrow, developed sandy barrier island to hurricane forcing by addressing three main objectives (Figure 1.2). The study area for this work is Bay Head, NJ, USA, which was impacted by Hurricane Sandy on 29 October 2012. While neighboring borough Mantoloking located immediately south of Bay Head sustained major damage to buildings and roadways, Bay Head was protected by a buried rock seawall located beneath its dunes. As described in Chapter 2 and published in Smallegan et al. (2016), results from the numerical model XBeach (see Appendix A) show wave energy is absorbed by the dune, resulting in its deformation, until the peak of the storm. At that time, the eroded dune leaves the buried seawall uncovered, such that the seawall

blocks waves from attacking subaerial portions of the island throughout the remainder of the storm. Compared to Mantoloking not fronted with a seawall, Bay Head's seawall reduced wave attack by a factor of 1.7 and preventing bay side flooding, which caused a major erosive event in Mantoloking.

Since bay side flooding caused extreme erosion in the absence of a seawall, the effects of bay surge on barrier island morphology is investigated in Chapter 3. While maintaining Hurricane Sandy offshore wave and surge conditions, the timing and magnitude of peak bay surge is altered and the morphological change in the presence and absence of a seawall re-simulated. For all bay surge conditions, the seawall becomes uncovered during the storm and prevents severe lowering of backbarrier elevations. However, in the absence of a seawall, shifting the occurrence of peak bay surge such that it coincides or precedes peak ocean surge prevents severe erosion on the backbarrier and reduces erosion on the dune. Although bay surge magnitude and erosion are found to have a direct relationship as expected, the relationship is not proportional. Decreasing bay surge magnitude results in relatively large reductions in backbarrier erosion, whereas increasing magnitude causes only moderate increases in erosion.

In order to protect the barrier island from future rises in sea level, which affects ocean and bay storm surge levels, several adaptation strategies to future SLR are evaluated in Chapter 4. Considering ten strategies, including combination nature-based and hard structures, and three SLR scenarios, morphological change of the barrier island is simulated. Overall, increasing beach and dune elevations relative to SLR offers additional protection over the "Do-Nothing" strategy for low to moderate SLR but exacerbates backbarrier erosion for extreme SLR. Of the strategies considered, raising island elevations is the only option able to protect the barrier from moderate to extreme SLR by reducing erosion on the dune and backbarrier regions.

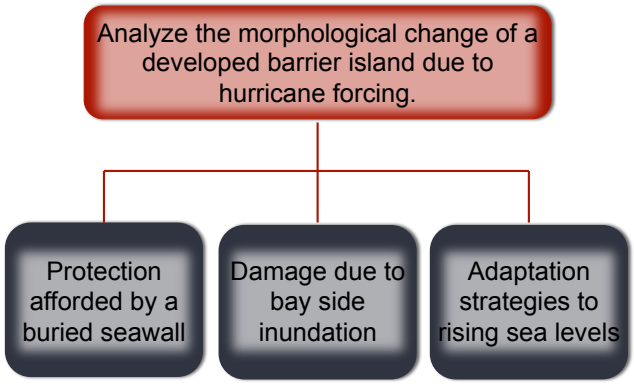

Figure 1.2: The overall purpose of this study consists of three main objectives, which are addressed in Chapters 2–4.

Chapter 2

Morphological response of a sandy barrier island with a buried seawall during Hurricane Sandy

Stephanie M. Smallegan[1], Jennifer L. Irish[1], Ap R. Van Dongeren[2], Joost P. Den Bieman[2]

[1]Department of Civil and Environmental Engineering, Virginia Tech, Blacksburg, Virginia 24061, USA
[2]Deltares, Delft, Netherlands

Reprinted from *Coastal Engineering*, volume 110, Stephanie M. Smallegan, Jennifer L. Irish, Ap R Van Dongeren, Joost P. Den Bieman, Morphological response of a sandy barrier island with a buried seawall during Hurricane Sandy, pages 102 – 110, Copyright 2016, with permission from Elsevier (see Appendix C for License Agreement).

2.1 Abstract

Coastal populations continue to increase globally, causing potential damage costs of coastal hazards to rise and community resiliency to become a worldwide priority. Recently, Hurricane Sandy (2012) devastated areas of New York and New Jersey and caused overwash and breaching of several urbanized barrier islands along the U.S. eastern seaboard. This study focuses on the morphological response of Bay Head, NJ, a township on a barrier island fronted with a buried seawall. The hydrodynamics and morphology of Bay Head during Hurricane Sandy are simulated with XBeach, a numerical model designed to study these processes during storm events. From the simulations, the seawall protected Bay Head by effectively dissipating wave energy during the peak of the storm and from rapidly increasing bay water levels that flood the backbarrier region of the island. When the seawall is removed from the simulation, dune heights are lowered, allowing bay side flooding to cause a devastating erosive event that completely destroys the remaining dune system. XBeach indicates severe erosion seaward of oceanfront buildings in the absence of a seawall (vertical erosion under the dune peak about 15 m more than in the presence of the seawall), and wave energy propagates further inland even after the storm has passed. However, with the seawall present, wave attack is reduced on the island by a factor of 1.7 and prevents bay side flooding from causing significant morphological change on the island. Therefore, the seawall increased resiliency of the Bay Head community during and after peak Hurricane Sandy forcing by preserving the dune system.

2.2 Introduction

Globally, coastal populations continue to grow, further increasing the need to develop sustainable communities resilient to coastal hazards (Hinrichsen, 1999; Neumann et al., 2015; Small and Nicholls, 2003). In 2000, an estimated 10% of the world's population lived in coastal zones with elevations of less than 10 m above sea level, which are highly vulnerable to damage from waves and flooding (McGranahan et al., 2007). Because of the concentration of urban development in these areas, coastal populations are expected to continue to increase, leading to new infrastructure and higher potential costs due to coastal storm events. These costs include tangible and intangible losses, such as physical damage to infrastructure, ecosystem loss and degradation, business and social disruptions and loss of life (Donnelly et al., 2006; Escudero et al., 2014; Kraus and Wamsley, 2003). Smith et al. (2015) have shown that, in the U.S. from 1980 to 2014, 50% of the direct economic damage caused by natural disasters were due to tropical cyclones. In other words, costs of coastal hazards are nearly equal to the combined costs of all other major natural disasters, placing a significant burden on the U.S. economy.

By accurately predicting the behavior of developed coastal areas during storm conditions and coupling the results with appropriate risk analyses (Escudero Castillo et al., 2012), city

planners can make better-informed decisions on sustainable infrastructure development and protection measures. However, the precise extent of storm-induced beach erosion, especially along barrier islands, is currently difficult to predict. Barrier islands, which make up 6.5% of the world's open ocean coastlines (Stutz and Pilkey, 2001), are the mainland coasts' first line of defense against storms, but they are susceptible to severe damage by overwash and breaching.

Overwash deposits are the landward transport of sediment from its originating dune, which lowers dune heights and increases vulnerability to damage from subsequent storms. However, overwash fans can also create new habitat, including those for endangered or threatened species (Dennison et al., 2012). In extreme cases, breaching can occur, which is the formation of a channel across a barrier island. Breaching occurs most commonly on narrow islands with low frontal dune heights. It can destroy infrastructure as the channel is formed (Donnelly et al., 2006; Sallenger, 2000), but it can also reduce flooding from storm surge by equilibrating water levels on the ocean and bay sides (Kraus and Wamsley, 2003). Although both processes can have positive environmental and ecological impacts, they are often detrimental to urbanized coasts.

To reduce storm damage along sandy beaches, combinations of nature-based and hard structures, such as armored dunes, have been implemented in several locations globally because they are more cost-effective and environmentally sustainable with respect to the use of hard structures alone (Basco, 1998). Examples in the U.S. include Virginia Beach, VA (Basco, 1998, 2000; U.S. Army Corps of Engineers [USACE], 2008), Galveston, TX (Gibeaut et al., 2003), and Jekyll Island, GA (Yang et al., 2012, 2010). However, the force-reducing effects of these combination of nature-based and hard protection designs have not been quantitatively assessed in the field, since it is not possible to remove the structure, recreate the same storm conditions at that location, and compare island responses with and without a structure present. Some laboratory studies, as summarized by Kraus and McDougal (1996), indicated seawalls, which were exposed in most of the experiments, can cause localized increases in erosion, but the net volume of sediment transported was generally less or about the same for cases with a hard structure compared to cases without a hard structure. Morton (1976) qualitatively described erosion around a seawall near Panama City Beach, FL during Hurricane Eloise (1975), but the seawall's effectiveness as a protective structure was not assessed. Irish et al. (2013) described a buried seawall in Bay Head, NJ, which was exposed during the peak of Hurricane Sandy (2012). In their study, the seawall's effectiveness at reducing wave forces was assessed during the peak of the storm using a Boussinesq-type wave model, where the dune shape was static and the seawall was presumed to be exposed throughout the numerical simulations. This approach yielded a factor of two wave force reduction with respect to a "no seawall" case.

In this study, we aim to evaluate the storm force-reducing effects of a dynamic sandy dune with a buried seawall when subject to storm conditions. Specifically, we use the numerical model, XBeach, to simulate hydrodynamics and morphology of Bay Head, NJ under Hurricane Sandy forcing. We then analyze the morphological response of the barrier island and

the wave force reducing capabilities of the sandy dune and buried seawall as it becomes exposed during the storm. Expanding the work by Irish et al. (2013), the full duration of Hurricane Sandy and the resulting sediment transport are simulated here.

2.3 Methods

2.3.1 XBeach model description

To simulate hydrodynamics and morphology during Hurricane Sandy, we use the numerical model XBeach, version 4613 (Roelvink et al., 2009). The two-dimensional (2D) depth-averaged model resolves infragravity waves, which have been shown to be of importance in the dune erosion process (Roelvink et al., 2009; Van Thiel de Vries, 2009). XBeach is capable of seamlessly modeling all four dune impact regimes as defined by (Sallenger, 2000), and model skill has been demonstrated on barrier islands (Lindemer et al., 2010; McCall et al., 2010) and urbanized coasts (Nederhoff, 2014; van Verseveld et al., 2015) among others. XBeach is chosen as the most appropriate numerical model to use, because it has been extensively validated for simulating morphological change over complex 2D bathymetry, and coastal structures can be represented as hard, non-erodable layers.

To calculate low frequency and mean flows, the nonlinear shallow-water wave equations are used. The radiation stress gradients, F, are determined by solving a wave action balance equation, which is coupled with a roller energy balance equation. Sediment transport is modeled using a depth-averaged advection diffusion Van Rijn - Van Thiel de Vries equation where sediment entrainment or deposition is determined by the difference between the depth-averaged and equilibrium sediment concentrations (Van Thiel de Vries, 2009).

Because XBeach does not resolve individual waves or full three-dimensional processes, some processes are parameterized using specifiable parameter values. In this study, most of these parameters are set to published default values; therefore, only parameters that were changed are discussed here. Since short wave runup can have a significant effect on morphology at the beach face (Van Thiel de Vries, 2012), this physical process is activated in all simulations, and the wave runup calibration coefficient, *facrun*, is specified to be 0.8 (default is 1.0, range is 0 to 2.0). Also, *jetfac*, an option used to mimic turbulence production near hard structures, is specified as 0.1 (default is 0, range is 0 to 1.0). Lastly, parameter *facua*, which governs onshore transport, is set to 0.25 (default is 0.1, range is 0 to 1.0) to account for wave skewness in the model. The reader is referred to Roelvink et al. (2009) for full details of the XBeach model.

2.3.2 Hurricane Sandy

On 29 October 2012, Hurricane Sandy made landfall near Atlantic City, NJ (Figure 2.1) and devastated communities along the northeastern U.S. coastline. Hurricane Sandy originated from a tropical wave that entered the Caribbean Sea and intensified to a hurricane on 24 October. Prior to entering the Atlantic Ocean, the storm made direct landfall in Jamaica and Cuba. Then, on 29 October, the hurricane collided with a non-tropical weather system, locally known as a Nor'easter, which prevented Hurricane Sandy from moving offshore. Instead, the hybrid storm, often referred to as Superstorm Sandy, veered west making landfall in the U.S near Atlantic City, NJ at 23:30 GMT on 29 October (Blake et al., 2013).

The unusually large post-tropical storm had a radius of about 280 km, maximum sustained winds of 130 km/h, and a minimum pressure of 945 mb at landfall. Hurricane Sandy was also characterized by record storm surges and large waves lasting over several high tides (Blake et al., 2013; Irish et al., 2013). In total for the U.S., Hurricane Sandy caused 159 fatalities and damages are estimated as $67 billion (USD) (Smith et al., 2015), making it the second-costliest hurricane since 1900 (Blake et al., 2013). Other physical damages were severe dune erosion, overwash and breaching of several barrier islands, including Fire Island, NY, Assateague Island, VA and along New Jersey. Hurricane Sandy left over 8.5 million customers without electricity on the order of weeks to months after landfall, caused health concerns, such as upper respiratory symptoms and worsened chronic conditions, and psychological impacts, including anxiety, sleep disturbances and posttraumatic stress (Blake et al., 2013; Lowe et al., 2015; Subaiya et al., 2014). A total of 24 states were impacted by Hurricane Sandy, ranging from gusting winds over the eastern seaboard and the Great Lakes to heavy snowfall in West Virginia and North Carolina, causing severe disturbances to businesses, land and air transportation, and social aspects (Blake et al., 2013; Halverson and Rabenhorst, 2013).

2.3.3 Study area

This study focuses on Bay Head, a township located along a barrier island in New Jersey (Figure 2.1). This island is a product of rapid post-glacial sea level rise and consists of Holocene beach and estuarine deposits, which are easily mobilized by waves and currents (Department of Environmental Protection, 1999; The Richard Stockton Coastal Research Center [RSCRC], 2015). Because the island is narrow, low-lying and mildly sloping, it is particularly vulnerable to storm surges (RSCRC, 2012; Williams, 2013). Although small patches of vegetation exist on the island, they are unable to protect Bay Head from large scale overwash during storm events, as has been observed in other locations (Feagin et al., 2015; RSCRC, 2012).

To help protect the island, over half of the shoreline is fronted with a rock seawall buried beneath a sand dune. The 1260-m long structure was originally built in 1882 and was

extended in 1962 (Irish et al., 2013; Remington & Boyd Engineers, 1962). In 1992, the seawall became exposed during a major Nor'easter, but was restored to its buried state, where it remained until Hurricane Sandy's impact (RSCRC, 2012). It has been noted that structural damage from Hurricane Sandy was substantially worse in areas not fronted with the seawall (Irish et al., 2013; RSCRC, 2012). This study aims to use a dynamic model to quantify the wave reducing effects of and protection afforded the buildings by the sandy dune that covers the seawall and the seawall as it became exposed during Hurricane Sandy.

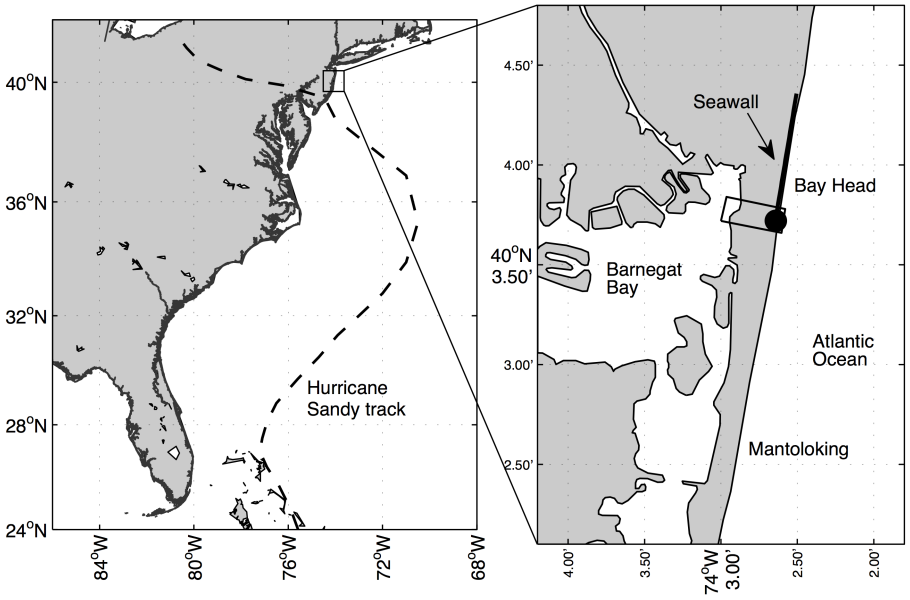

Figure 2.1: The study area is Bay Head, NJ (boxed, left panel) located north of Hurricane Sandy's landfall. Over half of Bay Head's shoreline is fronted with a buried seawall (solid black, right panel), and the area of interest modeled with XBeach extends northward 190 m from the south end of the seawall (boxed, right panel). An interior high water mark was measured as 4.6 m (black dot) within the area of interest (Irish et al., 2013).

2.3.4 XBeach model setup

Model grid

The 2D bathymetric grid used in all simulations (Figure 2.2 (a)) is developed using pre-storm surveys of Bay Head near the southern end of the seawall. The domain origin is 40.06°N, 74.05°W. Topography data are obtained from a U.S. Geological Survey (USGS) pre-storm first-return lidar survey, or "non-bare earth", collected in 2012 (USGS, 2012b) and a USACE pre-storm last-return lidar survey, representing the "bare earth", collected in 2010 (USACE, 2010). Since the 2012 bare earth data were not available at the time of this publication, the

2012 and 2010 data sets are combined such that the 2012 dune and shoreface are maintained, and 2010 bare earth data are used for all other island topography. This significantly reduces the noise caused by vegetation on the island, providing a more accurate representation of pre-storm conditions in Bay Head. In the nearshore region, one-dimensional (1D) cross-shore profiles surveyed by RSCRC (2012) are interpolated and merged with the 2D topographic grid. Barnegat Bay bathymetry is obtained from lidar data collected by USGS in October 2012 prior to Hurricane Sandy's landfall (Wright et al., 2014). All remaining bathymetry data, including offshore depths, are extracted from the National Oceanic and Atmospheric Administration (NOAA) Coastal Relief Model (National Geophysical Data Center, 2013). A representative cross-shore profile of the topographic and bathymetric relief is given in Figure 2.2(b), with the seawall location and shape shown in the inset.

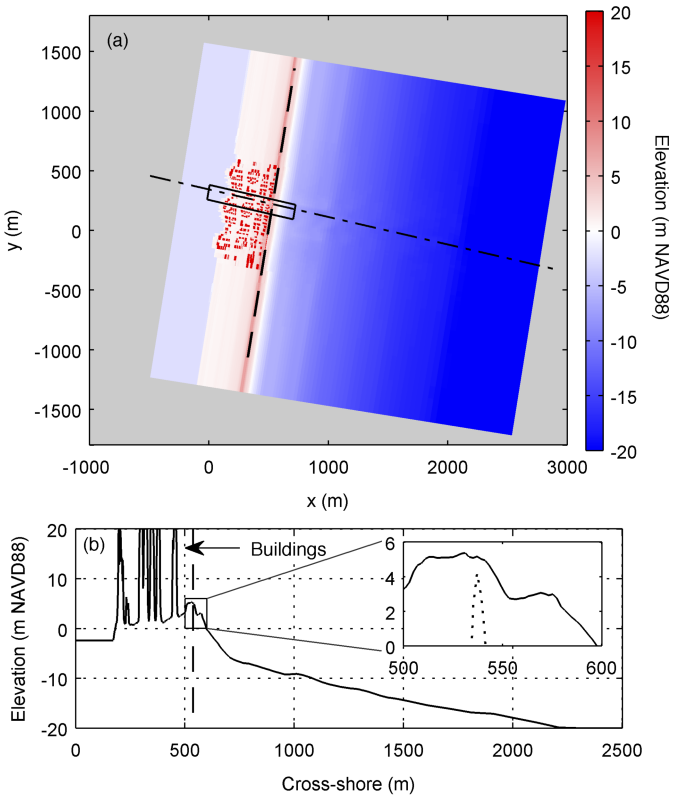

Figure 2.2: Data used for (a) the full model grid with cross-shore and longshore resolution ranging from 2 m to 50 m, (b) a representative cross-shore profile (dash-dot line in (a)) and the buried seawall in the inset. Buildings (red polygons) and the seawall (black dash line) are input as hard structures. The boxed region in (a) is the area of interest with origin coordinates of 40.06°N, 74.05°W.

Using satellite imagery available via Google Earth (Google, Inc., 2014), building locations

and shapes are determined and superimposed onto island topography. At the building locations, grid cells are set as 'non-erodable', or as hard structures that do not erode. If the hard structure grid cells become "wet", sediment transport over and sediment deposition on the structures are possible. It should be noted that hard structures are indestructible in the model, i.e., buildings are not damaged or destroyed in the simulations. The seawall is also set as a hard structure located at 4.45 m NAVD88, or about 2 m beneath the dune crest, with 1:1 side slopes (Remington & Boyd Engineers, 1962). Here, we have corrected the seawall elevation by accounting for sea level rise from 1962 to 2012 using the linear trend measured at a tide gauge in Atlantic City, NJ (4.08 mm/y) and converting from MSL to NAVD88 datum (NOAA Tides and Currents, 2015). The final grid resolution ranges from 2 m to 50 m in the cross-shore and longshore directions so that the seawall and buildings are sufficiently resolved.

Wave and surge data

In this study, Hurricane Sandy is modeled as a 74-hour storm beginning at 0030 GMT on 28 October 2012. Offshore spectral wave data are obtained from buoy 44025 (National Data Buoy Center, 2012). However, we observed energy in the low-frequency bands were truncated during the peak of the storm at some time steps. To account for this lost energy, the low-frequency data are fit with a linear trend extending from frequency bin 0.0425 Hz, the lowest bin likely to contain energy, to the spectrum peak. Although the total energy increase for those time steps requiring adjustment is only 7.5% and there is a negligible change in model results, the adjusted energy spectra are consistent with measurements at other time steps and are more typical of hurricane wave conditions. The adjusted spectra are then used to drive SWAN, a third-generation wave model (Booij et al., 1999), which is used to transform waves from the 40 m buoy depth to the 20 m offshore boundary of the XBeach grid, beyond which depth one can expect significant morphological change. This step greatly reduces the required XBeach grid size, thereby reducing computational time by about 50%.

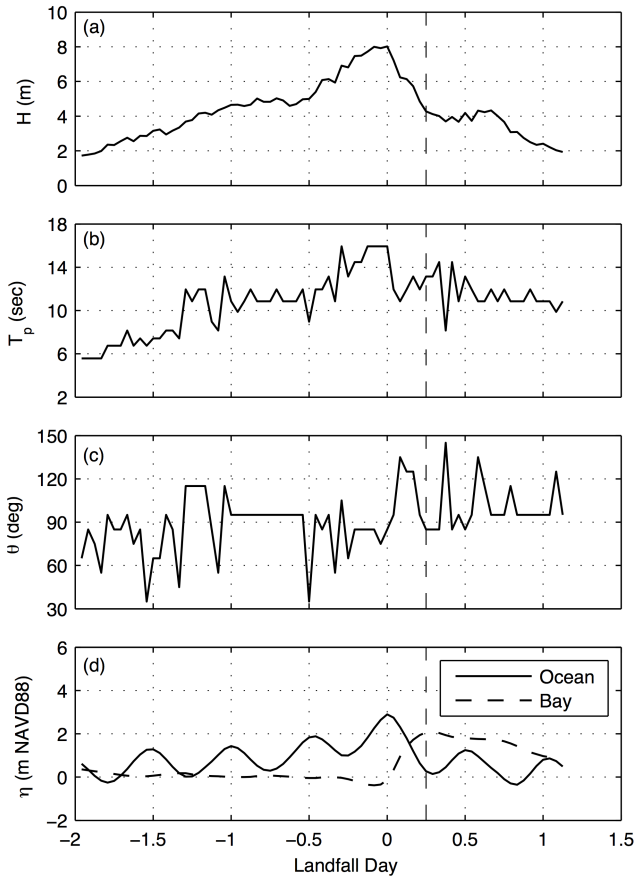

Figure 2.3: XBeach model inputs at 20-m depth for Hurricane Sandy: (a) wave height, H, (b) peak period, T_p, (c) wave direction, θ, in nautical convention and (d) water level, η, of the ocean (solid) and bay (dash). The vertical dash line distinguishes Phase 1 (left) from Phase 2 (right), and 0 (zero) landfall day is specified at 2330 GMT on 29 October 2012.

Figure 2.3 gives wave conditions at the offshore boundary of the XBeach grid, and shows (a) H reaches over 8 m, (b) T_p increases to 16 sec during the peak of the storm corresponding to sea swell, and (c) waves are typically shore-normal (100°) with some waves approaching from the northeast at the beginning of the storm and from the southeast as the storm passes.

Due to record high storm surges experienced during Hurricane Sandy, the tide gauge nearest to Bay Head failed during the peak of the storm. However, the Stevens Estuarine and Coastal Ocean Model (sECOM) (Orton et al., 2012) has been shown to accurately simulate Hurricane Sandy surge levels at several other tide gauges, including gauges located to the north of Bay Head in Sandy Hook, NJ and the Battery, NY and to the south of Bay Head in Atlantic City, NJ (Nederhoff, 2014). Therefore, sECOM-simulated water levels at the XBeach offshore boundary are used for ocean surge input (Figure 2.3(d)). Barnegat Bay water levels near Bay Head are from the USGS National Water Information System (2012)

gauge 01408168 (Figure 2.3(d)), which shows a 2 m increase within 8 hours after Hurricane Sandy's landfall.

Two phases of Hurricane Sandy impact are distinguished by the vertical dash line in Figure 2.3. Phase 1 occurs from the beginning of the simulation until 0.25 landfall day (6 hours after landfall) and is characterized by strong waves and ocean surge that exceed bay water levels. Phase 2 is characterized by weaker waves and bay water levels higher than ocean water levels. The impact of these phases on morphology are discussed in Section 2.4.2.

2.4 Results and Discussion

2.4.1 XBeach validation

Using the previously described data as input in XBeach, the hydrodynamics, sediment transport and morphological change near the southern end of the seawall in Bay Head are modeled for Hurricane Sandy conditions. The south end of the seawall is chosen because the island width is relatively narrow and backed by Barnegat Bay at this location, allowing overwash and breaching to become possible and bay side hydrodynamics to affect island response. This area also provides robustness to the model validation. Several studies have validated XBeach on natural systems absent of infrastructure (e.g. McCall et al. (2010)), but our study area includes a buried seawall, around which XBeach must accurately simulate morphological change. The pre-storm model input is shown in Figure 2.4(a), and the grid has been rotated such that the seawall is located at x=533 m. To validate the model setup, the post-Sandy first return lidar survey (Figure 2.4(b)) completed by USGS on 05 November 2012 (USGS, 2012a) is compared to the final simulated island topography (Figure 2.4(c)). Although bare earth is not available, this data set is chosen for comparison because it was collected prior to the extensive human interaction immediately following the storm, namely re-burial of the seawall with sand. Thus, these data provide the most accurate post-storm survey, even though the data consist of significant noise caused by vegetation (Figure 2.4(b)).

In addition to comparing simulated to measured morphological change, the model setup is validated by comparing maximum simulated water levels to a high water mark collected during a post-storm field survey (Irish et al., 2013). XBeach simulates a maximum water level of 4.8 m, which is comparable to the interior water mark elevation measured in Bay Head of 4.6 m.

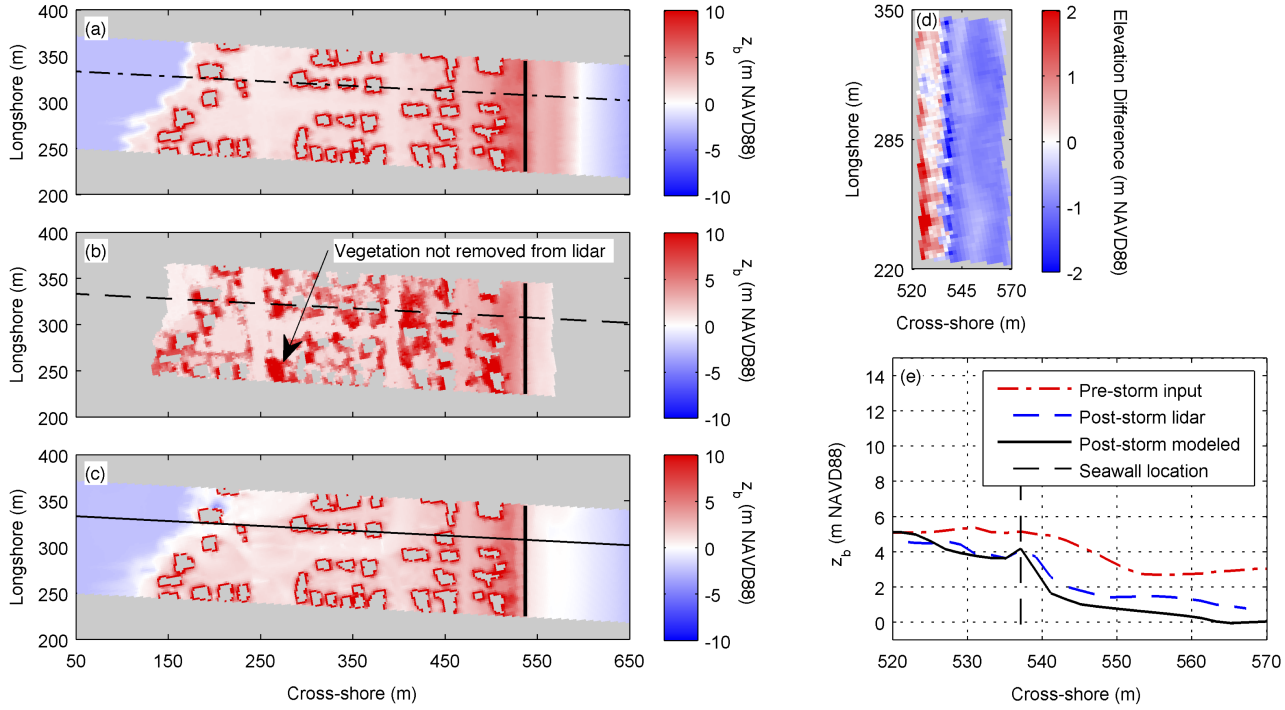

Figure 2.4: Data in the model domain: (a) elevation, z_b, of the pre-storm model input, (b) z_b of the post-storm first return lidar survey where red patches are vegetation that were not removed in the data set, and (c) z_b of the final XBeach result (seawall, black solid line); (d) elevation difference, Δz_b, between the final XBeach result and measured data (XBeach - lidar) for the dune and beach face region; (e) cross-shore profile (dash-dot line in (a), dash line in (b) and solid line in (c)) of pre-storm measurements (dash-dot), post-storm measurements (dash) and final XBeach result (solid). Building locations are shown in gray and domain origin is 40.06°N, 74.05°W.

Due to noise in the lidar data, only the area around the seawall is considered for quantitative analysis to validate the model setup. For this area, the difference between the XBeach result and lidar data is shown in Figure 2.4 (d), such that cooler colors indicate areas of lower simulated elevations by XBeach. Overall, the measured and modeled data appear to be in good agreement, except for the seaward side of the seawall, where XBeach simulates more erosion than observed in lidar data. The model performance is evaluated using the Brier Skill Score (BSS) method described by Van Rijn et al. (2003):

$$BSS = 1 - \frac{\langle (|z_{b,c} - z_{b,m}| - \Delta z_{b,m})^2 \rangle}{\langle (z_{b,0} - z_{b,m})^2 \rangle} \tag{2.1}$$

where $z_{b,c}$ is computed bed level, $z_{b,m}$ is measured bed level, $z_{b,0}$ is initial bed level, $\Delta z_{b,m}$ is the error in measured data equal to 0.20 m (USGS, 2012a), and $\langle ... \rangle$ represents the average

value. With this scale, a BSS equal to 1 indicates perfect model performance, a value of 0 means that the model performs as well as if no change were predicted, and a negative value means the model performs worse than predicting no change.

For areas around the dune and beach face, the BSS is 0.86, corresponding to "excellent" model performance as defined by Van Rijn et al. (2003). The bias is -0.65 m, which means XBeach overpredicts erosion, specifically on the seaward side and on top of the seawall. This bias has the same order of magnitude as prior work on a sandy barrier island (McCall et al., 2010) despite our study area being a built environment. There are several possible causes for this difference. Most notably, the seawall is assumed to have a uniform height in simulations, which may not be true of the rock structure in Bay Head. Also, the rock seawall allows some flow between its stones, but XBeach is currently unable to resolve this complex process. Instead, XBeach uses some of the incoming wave energy to simulate turbulence at the toe of the structure, which causes erosion on the seaward side of the seawall. Lastly, the beach face had been reworked by waves and several tidal cycles by the time the lidar survey was conducted, which may have caused sediment deposition in this area.

To provide a more detailed assessment of the results, data are extracted along the dash-dot, dash and solid lines in panels (a), (b) and (c) and plotted in Figure 2.4(e). The pre-storm dune height is significantly eroded during Hurricane Sandy, and the simulated result is in good agreement with measurements. For comparison purposes, this representative profile has a BSS of 0.89 and a bias of -0.56 m, which are similar to the BSS and bias of the region around the seawall.

2.4.2 Morphological response in the presence and absence of a seawall

To evaluate the morphological response of Bay Head in the presence and absence of a seawall, the seawall was removed from the previously described model setup and the storm re-simulated. From XBeach simulations, morphological change is substantially different in the two phases described in Section 2.3.4. By the end of Phase 1, wave attack and ocean surge cause erosion of the dune in the "seawall" case (Figure 2.5(a)) to the extent that the seawall becomes slightly exposed. A discussion on the temporal evolution of the dune profile is given below. In the "no seawall case", erosion is more severe due to island overwash, which causes the formation of channels through the dune and between buildings (Figure 2.5(b)). Figure 2.5(c) shows the elevation difference between the "seawall" and "no seawall" cases at the end of Phase 1, which is relatively small (+/- 1 m) except for the formation of these channels.

In Phase 2, a maximum of only 1 m of additional erosion occurs on the island in the presence of the seawall (Figure 2.5(d)). However, Figure 2.5(e) shows catastrophic island inundation, where erosion with a maximum of 6 m occurs at the dune peak and oceanfront buildings.

Also, the channels formed during Phase 1 are deepened and widened during Phase 2, and the back barrier region is eroded to an average elevation of -1.5 m NAVD88. Figure 2.5(f) shows elevation of the "no seawall" case is typically about 3 m less than the "seawall" case, with a maximum elevation difference of 15 m. This large difference is due to erosion of the dune itself, which has an initial height of at least 6 m in the study area, and severe erosion in front of the first row of houses.

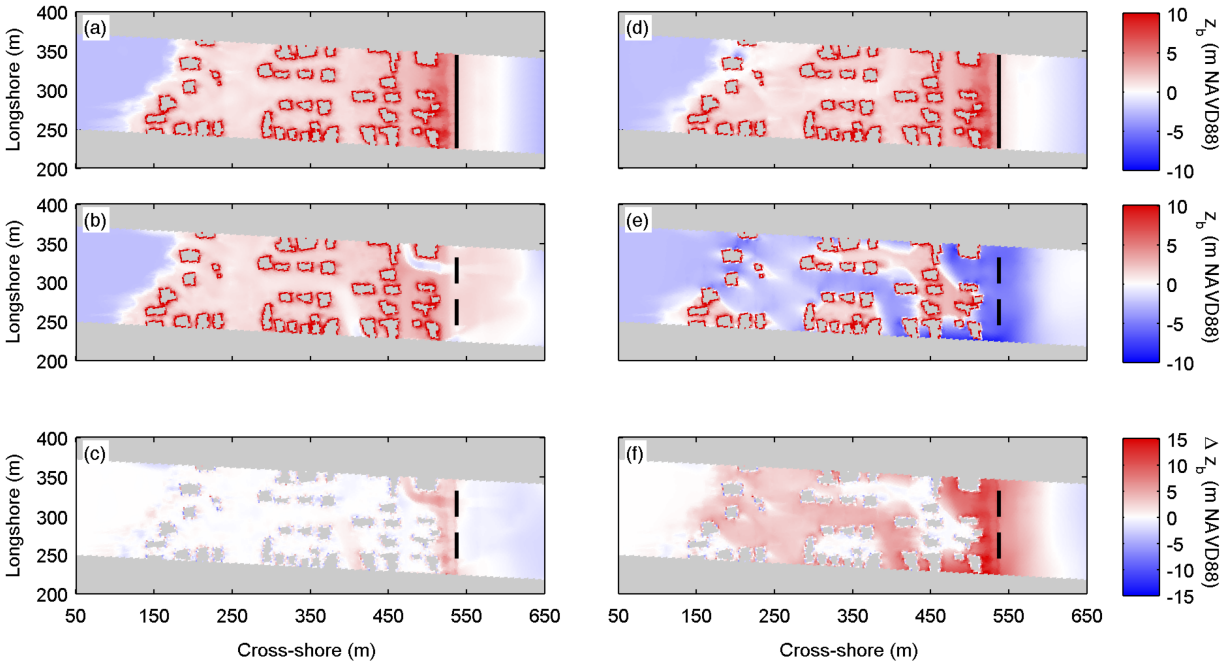

Figure 2.5: XBeach simulated bed levels: at the end of Phase 1 (a) "seawall" case, (b) "no seawall" case and (c) elevation difference, Δz_b, ("seawall" - "no seawall"); at the end of Phase 2 (d) "seawall" case, (e) "no seawall" case, and (f) Δz_b ("seawall" - "no seawall"). The solid lines represent the seawall location and the dash lines show the location of the removed seawall. Building locations are shown in gray and domain origin is 40.06°N, 74.05°W.

The wave reducing effects of the dynamic sandy dune and buried seawall are quantified by analyzing the time evolution of wave force per area, F_x (radiation stress gradient, dS_{xx}/dx, hereafter denoted as "force") along the representative profile in Figure 2.4 for the "seawall" and "no seawall" cases. This is shown in Figure 2.6(a) and (b). The storm impact regimes defined by Sallenger (2000) are used to evaluate Bay Head's morphological response to Hurricane Sandy and describe dune failure. These regimes are defined in terms of morphological change as follows:

- Swash (S) - beach foreshore, or the region seaward of the dune and berm, erodes and sediment is deposited offshore,

- Collision (C) - toe of the dune erodes and sediment is deposited offshore,
- Overwash (O) - dune crest is overtopped and sediment is deposited landward,
- Inundation (I) - island is submerged and sediment is deposited further landward.

Initially, the island is in the swash regime since only the beach foreshore erodes. As waves become larger and ocean water levels increase, the dune begins to erode, which is characteristic of the collision regime. The sandy dune dissipates wave force until approximately 2.5 hours prior to Hurricane Sandy's landfall. At that time, the seawall becomes exposed, is slightly overtopped signifying the overwash regime, and is heavily impacted by maximum wave forces of nearly 2000 N/m^2. Because of the seawall, much of the dune system is preserved and wave force does not inundate the dune peak as the storm passes. However, in the absence of the seawall (Figure 2.6(b)), wave force propagates nearly 80 m further inland due to significant dune erosion during the peak of the storm, and the island enters the inundation regime. After the storm passes, wave force continues to propagate onto the island, since the dune is destroyed and no longer protects the island from wave action.

In Figure 2.6(c) and (d), the time evolution of elevation change behind the seawall is shown for the representative cross-shore profile of the "seawall" and "no seawall" cases. In the presence of the seawall, no sediment is transported over the seawall prior to Hurricane Sandy's landfall. At the peak of the storm (t=0), about 1 m of sediment is eroded from behind the seawall, but no additional bed level change occurs for the remainder of the storm. However, in the absence of the seawall, over 3 m of erosion occurs at the dune peak when Hurricane Sandy makes landfall. Here, the distinction between Phases 1 and 2 can clearly be made at 0.25 landfall day due to the much larger erosive event (greater than 5 m dune erosion) caused by the sharp increase in bay water levels.

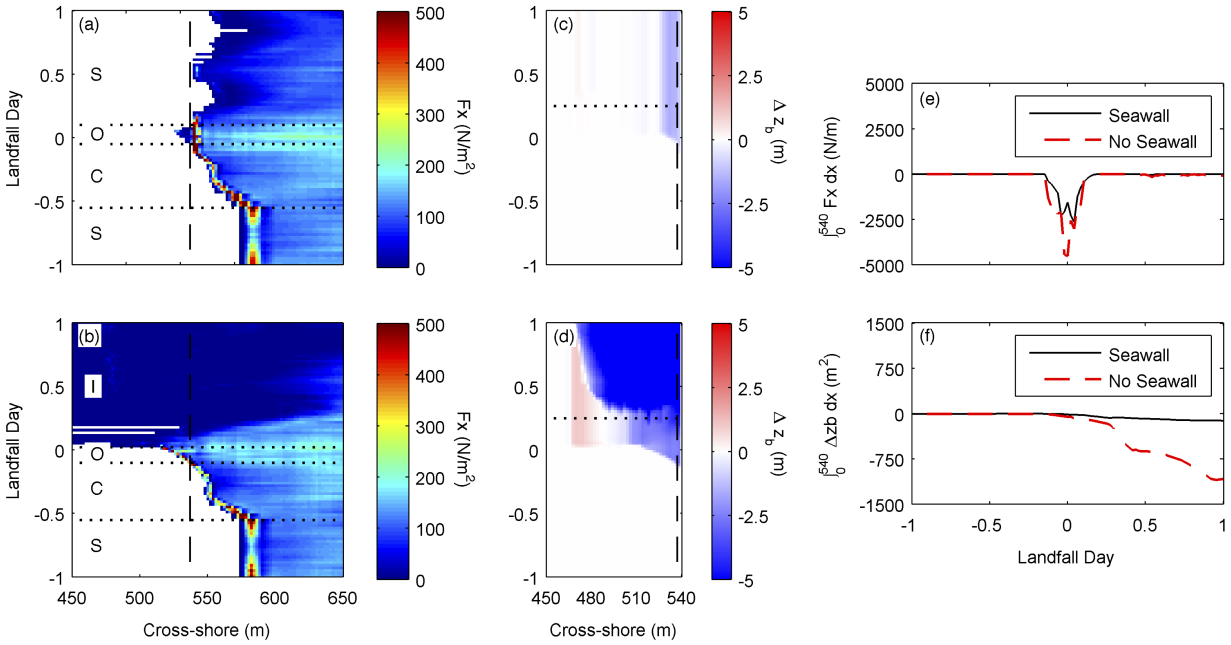

Figure 2.6: Time evolution with respect to landfall of Hurricane Sandy: (a) F_x in the presence of the seawall, (b) F_x in the absence of the seawall, (c) elevation change landward of the seawall location, Δz_b (final - initial), of the "seawall" case, (d) Δz_b of the "no seawall" case (cool colors indicate erosion), (e) integral of F_x over cross-shore distance landward of the seawall and (f) integral of Δz_b over cross-shore distance landward of the seawall (solid line is "seawall" case, dash line is "no seawall" case). F_x is the wave force per unit area in the cross-shore direction extracted along the profile in Figure 2.4, and 0 (zero) landfall day is specified at 2330 GMT on 29 October 2012. Dashed lines in (a) - (d) show seawall location, dotted lines in (a) and (b) indicate storm impact regimes (Sallenger, 2000), and dotted lines in (c) and (d) distinguish Phase 1 (bottom) from Phase 2 (top).

By integrating force and elevation change behind the seawall with respect to cross-shore distance, the wave force reducing effects of the seawall are analyzed. Figure 2.6(e) shows a significant reduction in wave force during the peak of Hurricane Sandy in the "seawall" versus the "no seawall" case. The maximum wave force reduction factor is 1.7, consistent with the findings of Irish et al. (2013) (maximum reduction factor of 2.0), even though XBeach and the Boussinesq model used in their study simulate physical processes differently. In Figure 2.6(f), the large erosive event in the "no seawall" case is clearly observed starting at about $t = 0.25$ landfall day, but there is no morphological impact on the "seawall" case at that time.

2.5 Conclusions

To evaluate the morphological response of a developed barrier island fronted with a buried seawall, the numerical model XBeach is used to simulate hydrodynamics and morphological response of Bay Head, NJ during Hurricane Sandy (2012). From these results, the seawall in Bay Head clearly served to protect coastal infrastructure and preserve the dune system during and after the storm. XBeach simulations indicate morphological change during two phases. In Phase 1, wave attack and ocean surge reach maximum values, and the seawall reduces wave forces by a factor of 1.7. In the absence of the seawall, dune heights are lowered, making the island vulnerable to wave action and flooding. During Phase 2, wave attack is small, but bay water levels increase rapidly over 2 m within 6 hours after Hurricane Sandy's landfall, exceeding ocean water levels. Although this bay-side flooding caused catastrophic erosion in the absence of the seawall (an additional 5 m of sediment eroded), no significant additional erosion is observed in the "seawall" case since the dune system remained in tact.

Although the results presented here are site and storm specific, the physical response of the sandy dune is realistic of other areas around the world with similar geology, i.e. narrow urbanized barrier island backed by a long narrow bay (Claudino-Sales et al., 2008; McCall et al., 2010; Sallenger, 2000; Silva et al., 2014). Therefore, we conclude the wave attenuation provided by the seawall is also physically realistic of performance of buried seawalls at other locations. Further investigations of armored dunes in other locations should be conducted under storm conditions to determine their possible benefit as protective structures. The feasibility of nature-based systems, such as additional beach nourishment or barrier island restoration, should also be evaluated since they can provide protection from flooding and breach formation without adding infrastructure to the beach (Cunniff and Schwartz, 2015; National Research Council, 2014). As identified by the present study, the effects of bay side hydrodynamics on morphological change of barrier islands are another topic of interest. Finally, some model limitations of this study include groundwater infiltration, rainwater runoff, and vegetation. These were not included in the simulations due to lack of available data or their relatively small effect on island morphology as observed from field data. Based on the reduction of across island erosion due to attenuation of wave forces by the sandy dune and seawall observed here, combination nature-based and hard structures may be a possible alternative for increasing coastal resiliency during storm events.

Acknowledgments

The authors thank Dr. Philip Orton, Stevens Institute of Technology, for providing surge data from sECOM simulations. This research was supported by NOAA Virginia Sea Grant Graduate Research Fellowship Program, National Science Foundation Graduate Research Fellowship program via grant number DGE-1148903, and National Science Foundation via grant number EAR-1312813. A. Van Dongeren and Joost P. Den Bieman were supported

through Deltares Research Program on "Hydro- and Morphodynamics during Extreme Events". The authors acknowledge Advanced Research Computing at Virginia Tech for providing computational resources and technical support that have contributed to the results reported within this paper. URL: http://www.arc.vt.edu.

Chapter 3

Barrier island inundation by bay side storm surge

Stephanie M. Smallegan[1], Jennifer L. Irish[1]

[1]Department of Civil and Environmental Engineering, Virginia Tech, Blacksburg, Virginia 24061, USA

The target journal for this manuscript is *ASCE Journal of Waterway, Port, Coastal and Ocean Engineering*.

3.1 Abstract

Barrier island overwash and breaching are caused by inundation from ocean surge and waves or from bay storm surge. According to a numerical model, a developed barrier island in New Jersey experienced a major erosive event during Hurricane Sandy (2012) due to an extreme rise in bay surge after the peak of the storm. In this study, a sensitivity analysis on the effects of peak bay surge timing and magnitude on morphological change in the presence and absence of a seawall is conducted. Results from the numerical model, XBeach, show the seawall protects the island from severe erosion by preventing ocean and bay surge from flowing freely across the island. In the absence of a seawall, the elevation of the island is greatly reduced during Hurricane Sandy conditions, and is exacerbated by increases in magnitude. However, shifting the timing or reducing the magnitude of peak surge reduces island erosion by up to 130% due to the bayward flow of ocean surge counteracting the seaward flow of bay surge.

3.2 Introduction

Barrier systems, particularly low-lying and narrow islands, are vulnerable to wave attack and flooding, especially during storms when water levels in the ocean and bay are elevated (Kraus and Wamsley, 2003). Of the world's open ocean coastlines, barrier islands comprise 6.5%, and most of the shorelines on the Atlantic and Gulf coasts are barriers (Gutierrez et al., 2007; Titus and Anderson, 2009). These barriers experience a variety of wind and wave climates, tidal forcing, and storm frequency and are backed by bays and estuaries with different shapes, sizes and number of tidal inlets (Titus and Anderson, 2009). They also have differing dune heights, island widths, sediment compositions and vegetation cover (Morton, 2002; Thieler and Young, 1991). Because of these differences, barrier island morphology during storms, which is dependent on seaward and bay side hydrodynamic forcing, is difficult to predict. The problem becomes more complicated on developed barrier islands where anthropogenic impacts must be considered.

Understanding the morphological change of barrier islands during storms is crucial for protecting coastal infrastructure from damaging erosion and scour, sustaining regional ecosystems dependent on periodic inlet formation and bay flushing, and the evolutionary progression of the barrier system to sea level rise (Gutierrez et al., 2007; Kraus and Wamsley, 2003; Titus and Anderson, 2009). Also, barrier islands are often the first line of defense to storms for the mainland coast and can reduce damages on the mainland by dissipating wave forces and blocking storm surge (National Research Council, 2014).

Although barrier islands have been the focus of many studies over the last several decades, predicting the response of a barrier to storm forcing, in a morphological sense, is still difficult due to a lack of fully understanding the governing processes. Since ocean surge and waves are

usually the most energetic forces during storm impact, damage is often estimated based on oceanic forcing (see Section 3.2.1; Morton, 2002; Sallenger, 2000). However, elevated water levels in the bay can also cause severe erosion, including dune overwash into the nearshore region or barrier island breaching initiated from the bay side (Kraus and Wamsley, 2003). This results in damages to the barrier system and infrastructure existing on the island, but the severity of erosion due to bay side inundation is difficult to predict.

On completely submerged uninhabited islands, morphological change has been shown to increase as the water level gradient between ocean and bay increases (Sherwood et al., 2014). In other words, an increase in bay surge magnitude causes more erosion, particularly on the backbarrier region of barrier islands, for a given magnitude of ocean surge (McCall et al., 2010; Sherwood et al., 2014). Similarly, more erosion is observed on undeveloped barrier islands when peak bay surge occurs after peak ocean surge based on a sensitivity analysis using a parametric base storm (McCall et al., 2010). The relationship between bay surge, ocean surge and morphological change is currently unknown for a slightly inundated (i.e. not completely submerged) developed barrier island. Therefore, the objective of this study is to investigate the effects of varying bay surge on erosion sustained by a barrier island during a hurricane in order to better predict the severity of erosion and damage on developed barrier islands. We hypothesize that barrier island morphological change becomes more severe as bay surge magnitude increases and when peak bay surge occurs after peak ocean surge.

The results of this study will enable coastal planners to develop sustainable ways to protect barrier islands from erosion caused by bay surge inundation, in addition to oceanic forcing. Nature-based, hard structures and combinations of nature-based and hard structure designs have been implemented on barrier islands to fortify them against storms (Basco, 1998; Kraus and McDougal, 1996; Pilkey and Wright III, 1988). In this study, we consider a buried rock seawall for reducing storm impacts. Located beneath the nourished dunes of Bay Head, NJ, USA, a rock seawall protected the developed barrier island from storm surge and waves and severe erosion caused by bay side flooding during Hurricane Sandy (2012; Irish et al., 2013; Smallegan et al., 2016). In the absence of the seawall, the island was severely inundated and experienced a major erosive event due to bay side flooding after the peak of the storm (Smallegan et al., 2016). By simulating morphological change of this developed barrier island to hurricane forcing using a numerical model, the effects of bay storm surge timing and magnitude on the island's morphological change are determined in the presence and absence of the buried seawall.

3.2.1 Storm impact regimes on barrier islands

During storms, barrier islands undergo significant morphological changes, described by Sallenger (2000) in four impact regimes, which are driven by ocean-side processes. The swash regime is characterized by sediment transported from the beach foreshore and deposited offshore but within the accessible sediment supply. Following swash is the collision regime

where the berm and dune are impacted by ocean surge and waves, often causing scarps and sediment deposition outside the region of available sediment supply.

The next two regimes, overwash and inundation, represent severe storm impact as dunes are overtopped and the island is flooded (Sallenger, 2000). On wave-dominated barrier islands, which are long narrow landforms where wave energy dominates tidal energy, overwash during storms is common (Gutierrez et al., 2007). Overwash is the landward transport of sediment from its originating dune. The inundation regime is the most severe impact regime in which ocean surge and waves impact the subaerial regions of the barrier island (Sallenger, 2000). In extreme conditions, breaches are formed which are channels that develop across the island and can destroy coastal infrastructure on developed barrier islands (Kraus and Wamsley, 2003; The Richard Stockton Coastal Research Center [RSCRC], 2012).

3.2.2 Barrier island inundation by bay side flooding

Although breaches formed during the inundation regime are, by definition, due to ocean-side inundation, breaches can occur from the bay side when bay water levels increase due to high local surge, precipitation and surface water runoff into the bay, and water level setup due to wind (Kraus and Wamsley, 2003). Data showing a bay-to-ocean breach are extremely difficult to obtain due to the unpredictability of breach formation and location, the occurrence of an intense storm during data collection, and a storm landfall location able to produce conditions for bay side inundation. However, Sherwood et al. (2014) measured seaward sloping water levels on Chandeleur Islands in the Mississippi Delta, USA from wind generated water level setup in the bay during Hurricane Isaac (2012). According to the in situ data and results from a numerical study, the water level gradient caused a breach to form through the low-lying undeveloped barrier island chain (Sherwood et al., 2014). Examples of other locations in the U.S. known to have breached from bay side inundation, also called storm-surge ebb, are Moriches Inlet, NY (Kraus and Wamsley, 2003), Bolivar Peninsula, TX (Goff et al., 2010), Folly Island, SC (Lennon, 1991) and Bay Head, NJ (Smallegan et al., 2016).

All of the previous examples vary by amount of infrastructure development, local tidal range, and wind and wave climate, but each barrier island was impacted by a storm that produced bay surge conditions able to inundate the backbarrier region. Bay surge depends on several storm and topographical characteristics, including storm path, landfall location, and shape of the bay that backs the barrier island (Rego and Li, 2010; Sheng et al., 2010). Because of the complexity of each location and storm, large-scale predictors of bay inundation on barrier islands require simplification of the barrier system and storm inputs (Plant and Stockdon, 2012). Therefore, sensitivity analyses, such as this study, are useful for predicting the behavior of a given location for a broad range of possible storms and landfall locations, which produce varying bay surge. In this study, the effects of varying bay surge on morphological change is evaluated for Bay Head, NJ, USA, a developed barrier island inundated from both

the ocean and bay sides during Hurricane Sandy (2012; Smallegan et al., 2016).

3.2.3 Study area

Bay Head, NJ USA is located on a sandy barrier island backed by Barnegat Bay, a long narrow bay (Figure 3.1). It is a wave-dominated barrier island (Gutierrez et al., 2007) with the nearest inlet located about 33 km south of Bay Head and 50 km north of Hurricane Sandy's (2012) landfall location. During this storm, a 1260 m-long buried seawall located beneath the dunes in Bay Head (Figure 3.1) was uncovered and protected the island from the damaging impacts of wave forces (Irish et al., 2013; Smallegan et al., 2016). Locations south of Bay Head not fronted with a seawall experienced extreme overwash and breaching (RSCRC (2012)). By numerical modeling, we showed, after the peak of the storm and in locations without a seawall, bay side storm surge inundated the island and caused major erosion, which reduced backbarrier elevations to critically low levels (Smallegan et al., 2016). However, our simulations indicated the seawall blocked bay surge from flowing freely over the island and prevented sediment from being transported from the backbarrier into the nearshore region.

The model setup for Bay Head, described in detail in Smallegan et al. (2016), is used in this study to meet two main objectives: determine the extent to which the seawall protects the island from severe erosion due to bay side flooding; and determine the severity of erosion caused by varying bay surge magnitude and timing. The model domain (Figure 3.1 (b) – (c)) is located at the south end of the seawall in Bay Head where the offshore direction corresponds to the increasing x direction. Buildings (gray polygons; (Figure 3.1) (c)) and the buried seawall (dark gray; (Figure 3.1) (d) – (e)) are input as hard structures that cannot be damaged or destroyed in the simulation. However, sediment can be eroded or deposited on the structures and flow can be channelized due to the presence of the buildings.

During Hurricane Sandy, a tide gauge located 2.5 km south of the model domain (Figure 3.1 (b); (U.S. Geological Survey National Water Information System, 2012)) measured bay storm tide. The data revealed interesting characteristics of the bay surge due to Bay Head's proximity to the nearest inlet, the shape of Barnegat Bay, and the landfall location of Hurricane Sandy. Prior to storm peak, southerly winds pushed water to the southern end of the bay, causing water level setdown in its northern end near Bay Head (Figure 3.1). As the storm passed and wind direction shifted, a sudden increase in bay surge was measured. Water levels remained elevated for more than one day after storm landfall.

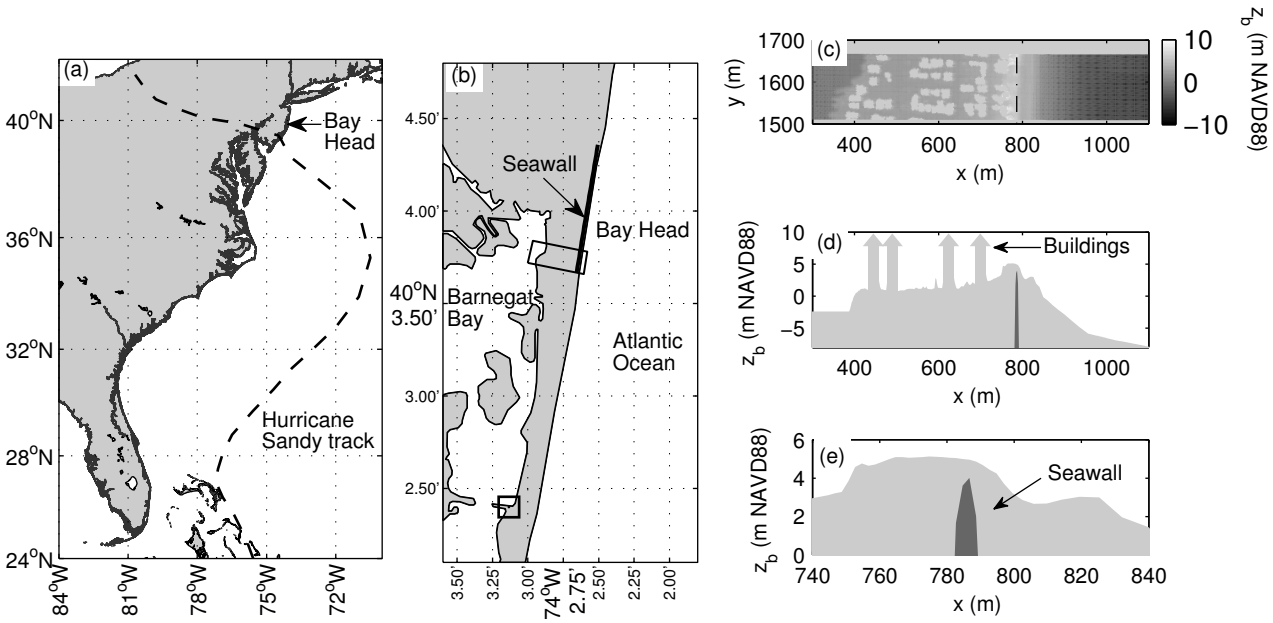

Figure 3.1: Locations of (a) Bay Head, NJ, USA relative to Hurricane Sandy's track; (b) the model domain (rectangle) and bay side tide gauge (box); (c) model domain (offshore is in increasing x direction; seawall is located at vertical dash line); (d) cross-shore profile through model domain; (e) cross-sectional area of buried seawall.

3.3 Methods

Using the numerical model, XBeach (Roelvink et al., 2009), the morphological response of Bay Head is simulated for Hurricane Sandy conditions and varying bay surge forcing. XBeach is a process-based model shown to simulate with high accuracy the morphological change of complex topography, such as barrier islands, during storm events (McCall et al., 2010; Roelvink et al., 2009). XBeach has also been used to evaluate the protection afforded by the buried seawall in Bay Head during Hurricane Sandy (Smallegan et al., 2016). Figure 3.2 shows the validation of the model setup, which is evaluated by comparing measured post-storm survey data to simulated morphological change to Hurricane Sandy. Using a Brier Skill Score (Van Rijn et al., 2003) to evaluate model performance, XBeach performs well with a score of 0.86 out of 1, where 1 indicates perfect model performance. By removing the seawall from the model setup and re-simulating Hurricane Sandy, XBeach results show the seawall reduced wave attack on the island during the storm by nearly a factor of two compared to locations without a seawall (Irish et al., 2013; Smallegan et al., 2016) and preserved the dune system which prevented bay side inundation (Smallegan et al., 2016).

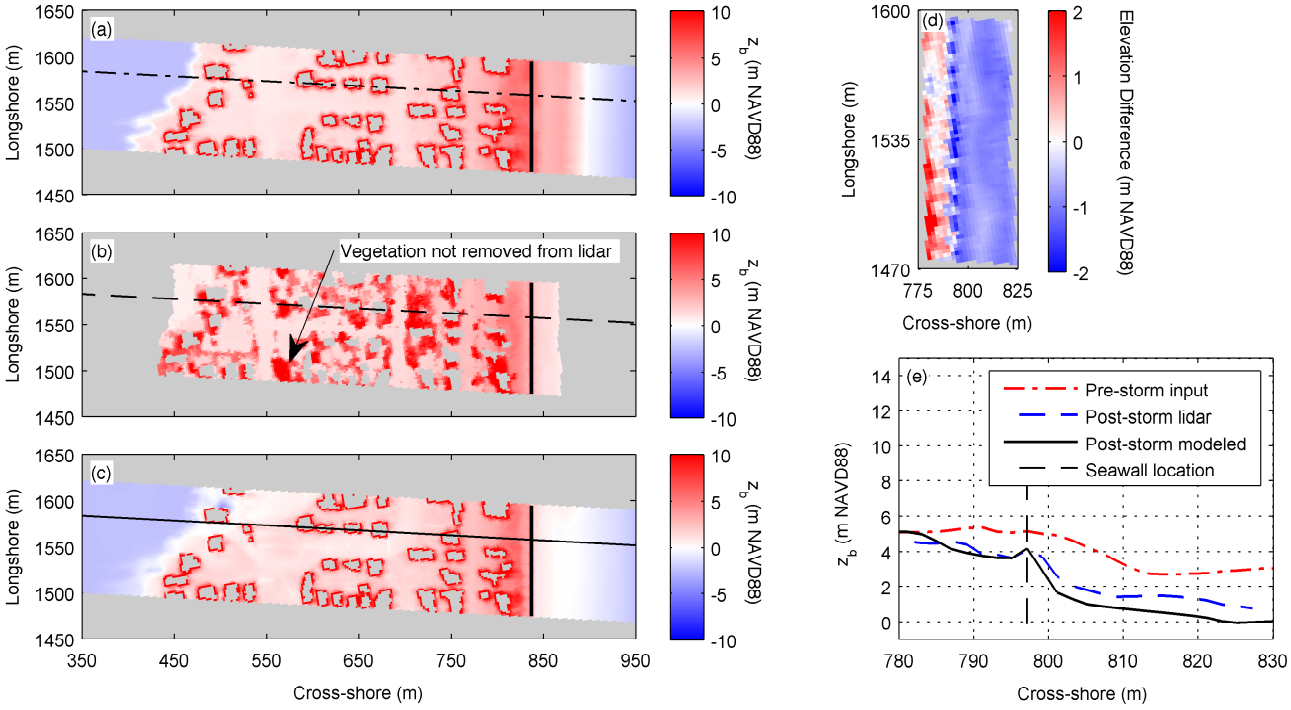

Figure 3.2: Data in the model domain: (a) elevation, z_b, of the pre-storm model input, (b) z_b of the post-storm first return lidar survey where red patches are vegetation that were not removed in the data set, and (c) z_b of the final XBeach result (seawall, black solid line); (d) elevation difference, Δz_b, between the final XBeach result and measured data (XBeach - lidar) for the dune and beach face region; (e) cross-shore profile (dash-dot line in (a), dash line in (b) and solid line in (c)) of pre-storm measurements (dash-dot), post-storm measurements (dash) and final XBeach result (solid). Building locations are shown in gray. Reprinted with permission (see Appendix C) from Smallegan et al. (2016).

In this study, relationships between island morphology and bay surge in the presence and absence of a seawall are determined using the model setup described by Smallegan et al. (2016). In all simulations, wave conditions and ocean surge (Figure 3.3 (a)) are maintained, whereas bay storm surge timing (Figure 3.3 (b)) and magnitude (Figure 3.3 (c)) are altered. According to numerical simulations of storm tide in the Gulf of Mexico and Galveston Bay during Hurricane Ike (2008), ocean surge remained relatively constant near the coast but surge magnitude in Galveston Bay varied by over 40% depending on location within the bay (Rego and Li, 2010). Considering sea level rise, Taylor et al. (2015) show amplification and deamplification of bay side storm surge in Panama City, FL by as much as +/- 15% due to changes in free surface gradients of surge.

Depending on bay geometry and storm characteristics, including landfall location relative to an area of interest, bay storm surge may vary in magnitude or the timing of peak bay surge

may be offset from peak ocean surge. Because of the complexity surrounding the prediction of bay surge relative to storm surge, the known hydrograph of bay surge during Hurricane Sandy is altered. As an example, shifting the timing or altering the magnitude of peak bay surge relative to ocean surge represents scenarios of variable storm characteristics that generate different bay surge hydrographs or of different locations along the bay.

In the present study, bay surge is shifted by -12 hr and -6 hr, such that the timing of peak bay surge precedes and coincides with the timing of peak ocean surge. A shift of +6 hr is included such that peak bay surge coincides with post-storm high tide. These are chosen based on the water level gradient generated between the bay and ocean and the extent to which the beach and dune are eroded by ocean-side processes prior to the sudden rise in peak bay surge. In addition to shifting the time of peak surge, bay surge magnitude is increased by 15% to 50% and decreased by 15% to 50% (Figure 3.3 (c)). These values are within the range of bay surge magnitude observed in Galveston Bay and Panama City.

Morphological change is simulated for each of the bay surge scenarios, including the No Change case (NC) where no adjustment has been made, and in the presence and absence of a seawall (herein defined as Seawall, SW, and No Seawall, NSW). Throughout the storm, volumetric bed level change, V, is calculated as

$$V(t) = \int_{y_1}^{y_2} \int_{x_1}^{x_2} |z_b(t) - z_{bi}| dx dy \tag{3.1}$$

where $z_b(t)$ is the simulated topography at time t and z_{bi} is the initial topography. The absolute value of bed level change is then integrated over the model domain from longshore locations y_1=1510 m to y_2=1660 m and cross-shore locations x_1 and x_2 with values dependent on the region of the island (i.e. dune or backbarrier) of interest (Figure 3.1 (c)). V is calculated as a proxy for damage for all bay surge conditions in the presence and absence of the seawall. Although the direct correlation between V and damage is not determined here, each condition (V_C) is compared to the No Change condition (V_{NC}), such that values of V_C above V_{NC} suggests more damage is likely to occur compared with damage observed during Hurricane Sandy.

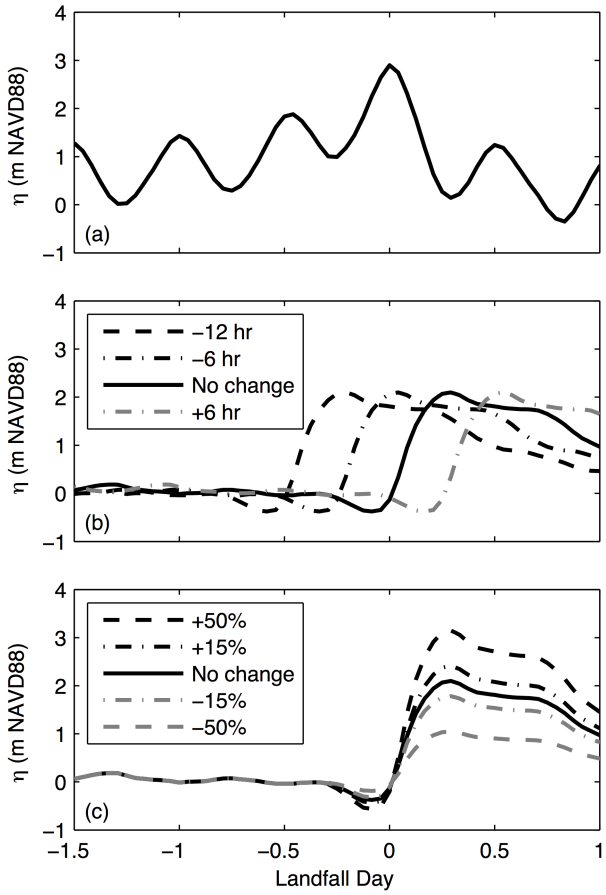

Figure 3.3: Time-varying water levels, η, of (a) ocean storm tide; (b) bay storm tide for Hurricane Sandy (black solid) and shifted by -12 hr (black dash), -6 hr (black dash-dot) and +6 hr (gray dash-dot); (c) bay storm tide for Hurricane Sandy (black solid) and +50% (black dash), +15% (black dash-dot), -15% (gray dash-dot) and -50% (gray dash) change in surge magnitude. Landfall day 0 (zero) is specified as 2330 GMT on 29 October 2012.

3.4 Results

Final simulation results are used to calculate V on the island (V_{island}: $x_1 = 380$ m, $x_2 = 840$ m), dune (V_{dune}: $x_1 = 725$ m, $x_2 = 840$ m), and backbarrier ($V_{backbarrier}$: $x_1 = 380$ m, $x_2 = 725$ m). Overall, shifting the hydrograph -12 hr, -6 hr or +6 hr causes relatively small changes in V ($< 5\%$ from the No Change case) in the presence of the seawall, but reduces bed level change for the No Seawall case by 17% to 130% (Figure 3.4 (a)). In the absence of a seawall, although reductions in mobilized sediment on the dune are observed (up to 78%), backbarrier bed level change is significantly reduced by up to 200% (-12hr and -6 hr).

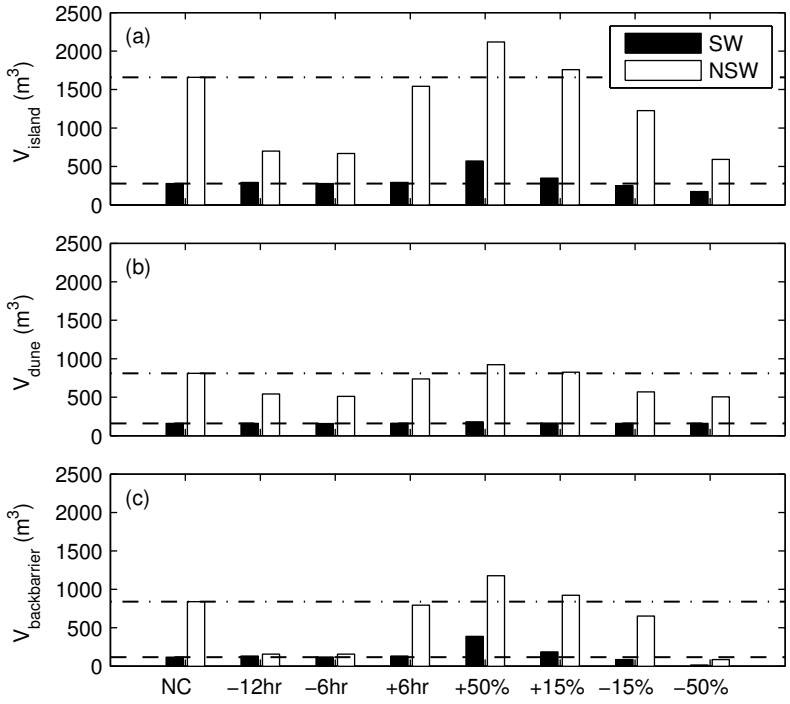

Figure 3.4: Change in sediment volume mobilized, V, for each alteration to bay surge on the (a) island (V_{island}: $x_1 = 380$ m, $x_2 = 840$ m), (b) dune (V_{dune}: $x_1 = 725$ m, $x_2 = 840$ m), and (c) backbarrier ($V_{backbarrier}$: $x_1 = 380$ m, $x_2 = 725$ m) for the seawall (black) and no seawall (white) cases. Values above the horizontal lines indicate more change in bed level than the No Change case for the Seawall (SW, dash) and No Seawall (NSW, dash-dot) cases.

To qualitatively show these changes in V for -6 hr shift, final bed elevations along a cross-shore profile are compared to the No Change condition (Figure 3.5). In the presence of the seawall, the time shift in bay surge causes a negligible change in morphological response. The dune remains in tact and the overall elevation of the backbarrier remains the same. However, for the No Seawall case, erosion in front of oceanfront buildings and on the backbarrier is greatly reduced compared to the No Change condition. The amount of sediment deposited in the nearshore region is also reduced.

As expected, increasing bay surge magnitude exacerbates sediment transport on the island, particularly in the backbarrier region (Figure 3.4). In the presence and absence of a seawall, for a +50% increase in surge, the volume of dune sediment mobilized increases by 6% and 30%, but backbarrier erosion greatly increases by 80% and 100% from the No Change condition. Backbarrier elevations are reduced in the Seawall case by an average 1.5 m from the initial profile and the back side of the dune is eroded (Figure 3.5 (a)). In the absence of a seawall, erosion in front of oceanfront buildings and on the backbarrier are exacerbated by the increase in surge (Figure 3.5 (b)).

Adjusting bay surge magnitude by +15% results in relatively small increases in mobilized sediment on the island (10% to 14%), mostly occurring on the backbarrier (19% to 25% more erosion than No Change in bay surge for this region) in the presence and absence of a seawall. However, a -15% decrease in bay surge magnitude causes a 60% reduction in overall erosion on the island for the No Seawall case. Final elevation of the dune is similar to that of -6 hr shift, but the backbarrier elevation is still significantly reduced to about -1.5 m NAVD88 (Figure 3.5 (b)). When bay surge magnitude is reduced by -50%, only small changes in V occur in the presence of a seawall, but V_{island} and $V_{backbarrier}$ are reduced by 145% and 220% in the No Seawall case (Figure 3.4).

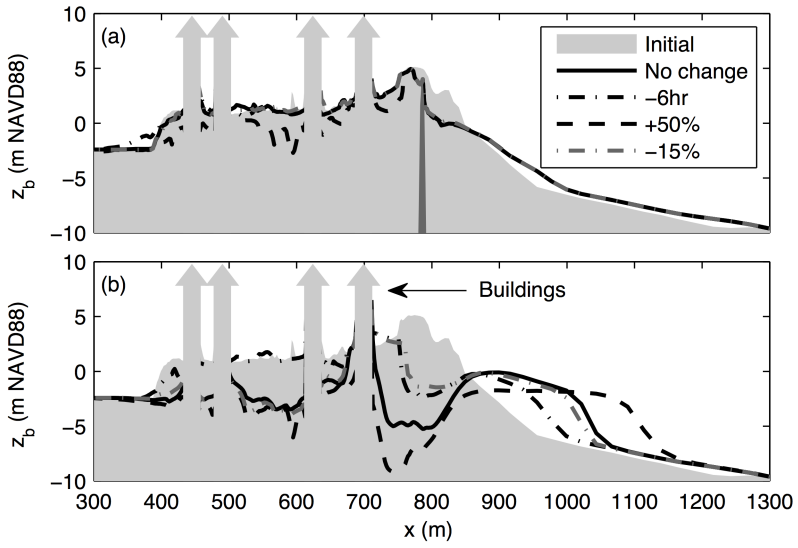

Figure 3.5: Cross-shore profile of final bed elevations, z_b, of the (a) seawall case and (b) no seawall case for No Change (black solid), -6 hr (black dash-dot), +50% (black dash), and -15% (gray dash-dot) alterations to bay surge. The initial profile (light gray shaded) and seawall (dark gray shaded) are shown for reference.

To analyze morphological change as the storm passes, temporal distributions of V are calculated on the island, dune and backbarrier for No Change, -6hr, +50% and -15% (Figure 3.6). In the presence of a seawall (Figure 3.6 (a)-(c)), -6 hr shift (similar to response of -12 hr; not shown) and -15% magnitude (similar to response of +6 hr shift; not shown) show nearly identical morphological change compared to the No Change condition as the storm passes. On the dune, V_{dune} shows very little increase prior to -0.45 days after landfall while in the swash regime (-1 to -0.45 days before landfall). As storm surge and waves become larger, the dune begins to erode characteristic of the collision regime (-0.45 to -0.05 days before landfall). The dune is only slightly inundated during the peak of the storm, and V_{dune} reaches its peak of about 40% mobilization of the sediment initially located on the dune. On the backbarrier, no sediment is eroded until the sudden increase in bay surge begins to occur (i.e.

$V_{backbarrier}$ is independent of ocean surge and waves for these simulated conditions). Because of the -6 hr shift, backbarrier erosion begins at about -0.05 days after storm landfall instead of 0.2 days after landfall as with No Change, +50% and -15%, but the shift does not lead to greater erosion. Increasing surge magnitude by 50% leads to 100% mobilization of sediment on the backbarrier (i.e. all sediment initially located on the backbarrier is eroded), which begins at the peak of bay surge (0.2 days after landfall) and $V_{backbarrier}$ reaches its peak at 0.8 days after landfall.

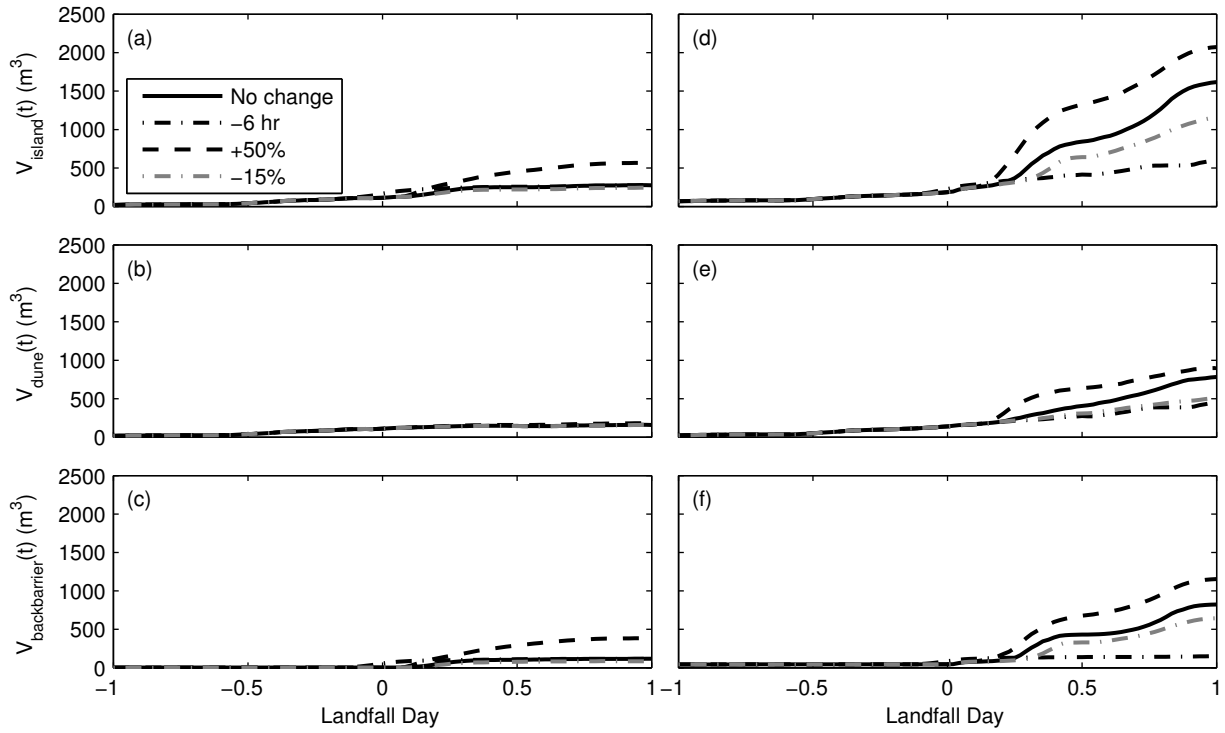

Figure 3.6: Time evolution of V for the seawall case on the (a) island, (b) dune, and (c) backbarrier; for the no seawall case on the (d) island, (e) dune, and (f) backbarrier for No Change (black solid), -6 hr (black dash-dot), +50% (black dash), and -15% (gray dash-dot) alterations to bay surge.

In the absence of a seawall, V_{island} steadily increases for all bay surge conditions, following similar trends for swash, collision and inundation regimes as the Seawall case, until 0.2 days after landfall when bay surge peaks (Figure 3.6 (d)-(f)). Since there is no seawall to prevent dune erosion, V_{dune} increases through the peak of the storm and experiences nonlinear increases for No Change and +50% conditions. At peak bay surge, No Change and +50% conditions cause sharp increases in sediment transport on island, and -15% shows a small but significant increase in V_{island}. Erosion continues with a linearly increasing trend for the -6 hr shift in bay surge. For -6 hr shift and -15% magnitude, V_{dune} increases linearly as the storm passes and is at least 63% lower by the end of the simulation than the No Change

condition in the absence of a seawall. Again, on the backbarrier, no sediment transport is observed until the sudden increase in bay surge (0.2 days after landfall; Figure 3.6 (f)).

Severe erosion is observed for all cases except the -6 hr bay surge shift, which has a similar morphological response as -12 hr and -50%. As the storm passes, $V_{backbarrier}$ remains constant and significantly lower compared to the No Change condition. The -15% magnitude in bay surge is still able to inundate the backbarrier causing a sharp increase in $V_{backbarrier}$ beginning at 0.35 days after landfall. For No Change, +50% and -15%, periods of sharp increases in backbarrier erosion correspond with high bay surge and low ocean surge and are followed by periods of lower sediment transport rates when bay and ocean surge are both elevated.

3.5 Discussion

Results from this study show two main conclusions: (a) minimizing ocean-side wave and surge impacts with a seawall also greatly minimizes the influence of bay flooding and (b) the timing of peak bay surge relative to peak ocean surge is critically important in governing the severity of damage sustained by the barrier island. This means that, for locations near Bay Head not fronted with a seawall such as neighboring borough Mantoloking, observed damages during Hurricane Sandy were more severe due to the timing and magnitude of peak bay surge, which relates to the location in the bay, and the lack of protection afforded by the seawall.

Overall, altering bay surge by shifting the timing or magnitude of peak surge causes relatively small changes in morphology compared to the No Change condition in the presence of the seawall but significant changes compared to the No Change condition for the No Seawall case (Figure 3.4). In the presence and absence of a seawall, nearly identical morphological responses were observed for all bay surge conditions until the peak of the storm. At that time, the seawall becomes exposed and blocks ocean surge and waves and preserves the dune system, whereas, in the absence of a seawall, V continues to increase (Figure 3.6; Smallegan et al., 2016). Specifically on the dune, V_{dune} was greatly reduced in the presence of the seawall compared to the No Seawall case. Previous work shows the seawall effectively protects the island against ocean waves and surge (Irish et al., 2013; Smallegan et al., 2016); however, here we show the structure also protects against bay side flooding. Because the seawall preserves the dune system behind it, bay surge inundation is not able to flow freely across the island. This, in turn, reduces erosion on the backbarrier compared to the No Seawall cases, even with significant increases in surge level (up to +50%).

Interestingly, shifting the timing of peak bay surge by -12 hr or -6 hr produces a similar response as reducing bay surge magnitude by -50% in the absence of a seawall. For these conditions, V_{island} decreases by 130% compared to the No Change condition, mostly due to reductions in $V_{backbarrier}$ of 200%. However, the causes of these responses are different between conditions. For -50% magnitude, bay surge levels do not exceed the minimum elevation of

the backbarrier; thus, bay surge is unable to inundate the island as observed in all other conditions. For -6 hr and -12 hr shifts, the resulting bed level difference compared to the No Change condition results from dunes remaining in tact at the time of peak bay surge and opposing flow directions across the island. As observed on uninhabited islands, in order for bay surge to inundate the island and significantly reduce backbarrier elevations, water from the bay needs to flow freely over the island, transporting sediment from the backbarrier into the nearshore region (Sherwood et al., 2014). Although the magnitude of bay surge is large enough to flood the backbarrier for -6 and -12 hr shifts, it is unable to inundate the dune system because dune heights have not been reduced by ocean surge and waves. As dune heights are lowered at the peak of the storm, the seaward flow from bay surge is opposed by the bayward flow from ocean surge thus, bay surge is not able to freely flow across the island. This results in significant reductions in V on the developed barrier island, following a similar trend as observed on undeveloped barrier islands in the Gulf of Mexico (McCall et al., 2010; Sherwood et al., 2014).

From XBeach simulations and along this cross-shore profile, -15% bay surge magnitude shows a similar morphological response on the dune as -6 hr time shift, but backbarrier elevations are greatly reduced with the lower magnitude (Figure 3.5). This is due to a breach that forms within the model domain (not shown) through which sediment is transported from the backbarrier to the nearshore region. Peak bay surge forcing coincides with low ocean surge after the peak of the storm (0.35 days after landfall), which causes the lower magnitude water levels to inundate the backbarrier and attack the backside of the weakened dune system. The breach forms at low points in the dune and provides a path of sediment transport without destroying the entire dune system (Figure 3.6 (b)). Therefore, -15% in bay surge magnitude serves as a threshold condition for the point at which the island is inundated but part of the dune system remains in tact.

As expected, altering bay surge magnitude was found to have a direct relationship with erosion; however, the relationship was not found to be proportionate. Increasing bay surge by +50% and +15% caused 63% and 13% more erosion compared to the No Change condition, whereas decreasing bay surge by -50% and -15% reduced erosion by 144% and 57% erosion. A similar trend was observed in a sensitivity analysis conducted during a numerical study of Santa Rosa Island, FL, USA during Hurricane Ivan (2004; McCall et al., 2010). Reducing bay surge magnitude by 25% caused a 35% reduction in backbarrier erosion, whereas a +25% bay surge increase caused a 15% increase. For higher levels of bay surge, which may be due to sea level rise or storm landfall location or intensity, the morphological change is expected to be less than observed under lower surge levels.

3.6 Conclusions

Using a numerical morphodynamic model, a sensitivity analysis on bay storm surge timing and magnitude is conducted for a developed barrier island during a hurricane. The morpho-

logical change of Bay Head, NJ, USA to Hurricane Sandy (2012) is simulated with XBeach. Then, bay storm surge is shifted by -12 hr, -6 hr and +6 hr, such that peak bay surge occurs prior to, at the same time as, and after peak ocean surge. Bay surge magnitude is also altered by +/- 15% and +/- 50%. Considering each of these alterations to bay storm surge, the morphological change of the barrier island in the presence and absence of a buried seawall, which is intended as a barrier to ocean-side storm forcing, is re-simulated.

Based on modeling results, the buried seawall reduces damage due to ocean storm surge and waves while also minimizing the impacts of bay side flooding. In the presence of a seawall, the dune system is preserved in all simulations and the post-storm elevation of backbarrier regions remain significantly higher compared to the post-storm elevations in the absence of a seawall. Results also show the timing and magnitude of bay storm surge relative to ocean surge is critically important for determining damage on developed barrier islands during hurricanes. When peak bay surge occurs after peak ocean surge, the dune systems are weakened by ocean-side surge and waves allowing bay side flooding to inundate and overtop the remaining dunes. This causes catastrophic erosion of the island, lowers the backbarrier to critically low elevations, and causes extreme erosion of the dune and in front of oceanfront buildings.

From this study, several recommendations about assessing the vulnerability of developed barrier islands and the corresponding engineering design of protection measures are made. Developed barrier islands, particularly those located on narrow bays in locations subject to water level setup (i.e. no nearby inlets), are vulnerable to bay side inundation and the damage caused by its erosion, while still being inundated by ocean surge and waves. Also, the timing of peak bay surge relative to ocean surge is important in determining the morphological change of the area of interest, which is related to its location within the bay. In this case, a buried seawall reduced the damaging effects of bay side flooding, as well as protected the island from ocean-side forcing. In the design of barrier island fortification against storm forcing, bay side hydrodynamics, as well as ocean-side impacts, must be considered. An engineering design intended to protect the island from only ocean wave and surge should be evaluated for the protection it will afford during periods of bay side inundation.

The limitations of this study include using one storm and study location for the sensitivity analysis of bay surge timing and magnitude. In future work, the present study should be expanded to include additional storms and developed barrier islands to further develop the relationships between bay surge and morphological change. Additional numerical investigations should be conducted on the Barnegat Bay region in order to predict the elevation of bay storm surge, depending on the location of storm landfall location and location within the bay.

Acknowledgments

This material is based upon work supported by the National Oceanic and Atmospheric Administration, U.S. Department of Commerce, via award number NA14OAR4170093 to Virginia Sea Grant; the National Science Foundation Graduate Research Fellowship Program via grant number DGE-1148903; and National Science Foundation via grant number EAR-1312813. The authors acknowledge Advanced Research Computing at Virginia Tech for providing computational resources and technical support that have contributed to the results reported within this paper, http://www.arc.vt.edu.

Chapter 4

Developed barrier island response to hurricane forcing under rising sea levels

Stephanie M. Smallegan[1], Jennifer L. Irish[1], Ap R. Van Dongeren[2]

[1]Department of Civil and Environmental Engineering, Virginia Tech, Blacksburg, Virginia 24061, USA
[2]Deltares, Delft, Netherlands

The target journal for this manuscript is *Climatic Change*.

4.1 Abstract

Over the last century, global sea levels have risen at a rate of 1.7 mm/yr and are expected to continue to rise in the future at a faster rate than previously recorded. In published scenarios, global sea level rise projections range from 0.2 m to 2.0 m by 2100 with some regions experiencing higher rise in relative sea level due to localized processes. As sea levels rise, low-lying barrier islands are threatened by episodic flooding and wave impact and are particularly vulnerable during storm events. In this study, we evaluate the effectiveness of several adaptation strategies, including combinations of nature-based and hard structures, on developed barrier islands to hurricane forcing under future sea levels. From results of a morphological numerical model, beach nourishment provides only slight increases in protection for the island from hurricane forcing as sea levels rise. Moreover, raising elevations of the dune or a buried seawall is effective at reducing overall volumetric erosion, but, under extreme sea level rise, the higher dunes and seawall exacerbates erosion in the backbarrier region due to bay side flooding. Of the adaptation strategies considered in this study, raising the elevation of the island, particularly the backbarrier region, offered the greatest protection from catastrophic erosion on the barrier island under future sea levels and hurricane forcing. Therefore, when considering adaptation strategies on developed barrier islands for protection against sea level rise, particular attention must be given to backbarrier elevations with respect to future bay flood levels.

4.2 Introduction

Although sea level rise (SLR) globally may reach critically high levels over the next century (up to 2 m; (Parris et al., 2012)), coastal communities are affected by even small changes in sea level. Low-lying areas are particularly vulnerable to damage from episodic flooding and wave forcing, impacting a greater amount of people globally as sea levels rise and landforms evolve (Crowell et al., 2010; Nicholls and Cazenave, 2010; Pachauri et al., 2014; Peduzzi et al., 2012; Williams, 2013; Woodruff et al., 2013). An estimated 10% of the world's population lives in these low-lying coastal zones with elevations less than 10 m above sea level (McGranahan et al., 2007). Therefore, it is imperative for coastal planners to develop adaptation strategies to protect infrastructure as sea levels rise (Nicholls and Cazenave, 2010; Pachauri et al., 2014; Parris et al., 2012; Peduzzi et al., 2012; Woodruff et al., 2013).

Barrier islands, which comprise 6.5% of the world's open ocean coastlines (Stutz and Pilkey, 2001), are sensitive to several forcing mechanisms, including waves, tides, and sea level changes (Gutierrez et al., 2007). As sea levels rise, it is possible for barrier islands to become unstable, which is characterized by rapid landward migration; decreases in island width, height, and sand volume; and increases in the frequency of overwash and breaching during storms (Gutierrez et al., 2007). For extreme SLR ($>$ 0.7 m by 2100 on wave-dominated barrier islands), it is very likely that a threshold condition will be reached, resulting in seg-

mentation of the island, amalgamation with the mainland, or transformation into a drowned (completely submerged) barrier island (Gutierrez et al., 2007; Titus and Anderson, 2009).

Historically, adaptation strategies, such as beach nourishment, the use of seawalls or combinations of these nature-based and hard structures, have been used to stabilize the morphological evolution of developed barrier islands as sea levels rise (Basco, 1998; Pachauri et al., 2014; Pilkey and Wright III, 1988; Titus and Anderson, 2009; U.S. Army Corps of Engineers [USACE], 2008). Beach nourishment effectively reduces the impacts of ocean-side flooding and wave attack during storm events, but the sediment is easily mobilized and periodic renourishment is required for beaches impacted by frequent intense storms (Cunniff and Schwartz, 2015). Also, oceanfront property owners often express concerns about property rights issues and ocean views being blocked by nourished dunes (Associated Press, 2015; National Research Council, 2014). Seawalls are permanent structures known to protect coastal infrastructure during periods of high wave energy (Irish et al., 2013; Pilkey and Wright III, 1988; Smallegan et al., 2016), but they can also exacerbate beach erosion (Kraus and McDougal, 1996; National Research Council, 2014; Pilkey and Wright III, 1988; Yang et al., 2012). These structures can be aesthetically unpleasing, reduce access to recreational beaches and provide a false sense of security in areas vulnerable to large waves and storm surge (Pilkey and Wright III, 1988). Hybrid nature-based/hard structures, such as a seawall buried beneath a nourished dune, have become attractive options for long-term stabilization of developed barrier islands because they combine benefits of both approaches while minimizing adverse impacts. However, none of these designs protect the island from back-bay flooding (National Research Council, 2014). Reclamation of bay side land will become necessary to reduce catastrophic erosion during storm events on low-lying barrier islands as sea levels rise.

In this study, we evaluate beach armoring, beach nourishment and bay side land reclamation as strategies for adapting to future SLR on developed barrier islands. Using a hydrodynamics and morphological model, the response of a nourished barrier island with a seawall buried beneath the dune in New Jersey, USA is simulated for a storm comparable to Hurricane Sandy (2012). We then consider several SLR scenarios, including past (from c1950), present (c2000) and future (to c2100), and evaluate the response of the sandy barrier island to rising sea levels and adaptation strategies.

4.3 Study Area

Bay Head is a borough located on a narrow barrier island in New Jersey, USA, and it is fronted with a seawall beneath a nourished dune (Figure 4.1). The seawall was originally built in 1882 with a length of 1260 m (Irish et al., 2013; Remington & Boyd Engineers, 1962; Salter, 2007). Throughout the early 20th century, the seawall remained buried with sand until a non-tropical storm, locally known as a Nor'easter, uncovered the seawall in 1962. While exposed, a series of seaward-extending groins were constructed and the beach under-

went major nourishment (Irish et al., 2013; Remington & Boyd Engineers, 1962). Another strong non-tropical storm impacted Bay Head in 1992, once again uncovering the seawall and causing the need for a second major beach nourishment (Irish et al., 2013; The Richard Stockton Coastal Research Center [RSCRC], 2012). The seawall remained buried beneath the dune until Hurricane Sandy (2012) impacted the area with record storm surges and large waves (Irish et al., 2013). Since the devastating impacts of Hurricane Sandy (2012), the seawall has been uncovered once more during a strong swell event generated by the offshore passage of Hurricane Joaquin (2015) (Associated Press, 2015; Mulshine, 2015).

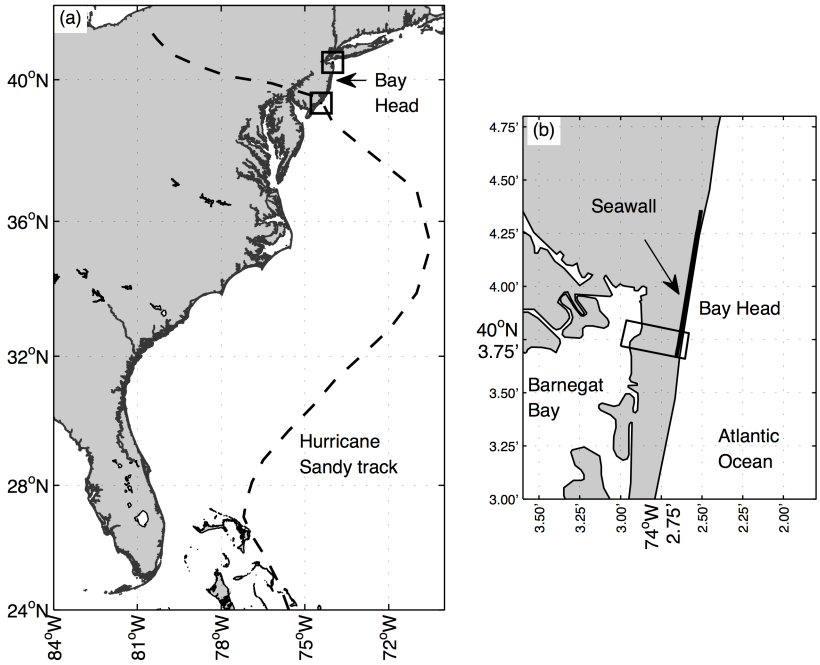

Figure 4.1: Location map of (a) Bay Head, NJ, USA and tide gauges (squares) in relation to Hurricane Sandys track; (b) the Bay Head seawall (heavy black) and model domain (rectangle).

4.4 Methods

4.4.1 Sea level rise historical trends and projections

In this study, we are interested in understanding the vulnerability of developed barrier islands to SLR. To this end, we consider in our analysis past SLR trends (c1950) and future SLR projections (c2100). SLR varies temporally and spatially and can be caused by thermal expansion, ice cap melting, vertical land movement (i.e. subsidence), and ocean circulation changes (Jevrejeva et al., 2008; McKay et al., 2011; Parris et al., 2012; Sallenger Jr et al., 2012; Yin et al., 2009). Globally, mean sea levels have risen by about 0.21 m since 1880, corresponding to a rate of 1.7 mm/yr (Church and White, 2011). Recent measurements from altimeter satellites show a higher global SLR rate of about 3.2 mm/yr for the period 1993 to 2008 (Ablain et al., 2009; Church and White, 2011). Sea levels are expected to continue to rise over the next century, but future SLR is extremely difficult to predict and much variation exists in published projections. For example, global SLR is projected to be at least 0.2 m and up to 2.0 m by 2100 and rise at a faster rate than previously recorded (Pachauri et al., 2014; Parris et al., 2012). Regional effects can cause relative SLR to be higher than the global rate, exacerbating the impacts of rising sea levels. Examples include Kushiro, Hokkaido, Japan and Grand Isle, Louisiana, USA, both of which are experiencing relative SLR rates of more than 9 mm/yr (NOAA Tides and Currents, 2015).

According to the historical mean sea level trend measured by tide gauges in New Jersey (Figure 4.1), the total relative sea level rise rate is 4.08 mm/yr, more than twice the observed global rate, based on data from 1911 to 2014 in Atlantic City (NOAA Tides and Currents, 2015). Data from 1932 to 2014 in Sandy Hook confirm this trend. Relative SLR in this area is caused by subsidence, mostly due to groundwater withdraw (Sun et al., 1999), although ocean circulation changes likely contribute to the measured trends (Yin et al., 2009). Using the historical sea level trend measured by the regional tide gauges, sea levels in c1950, which were about -0.2 m lower than present-day, are included in the analysis in order to compare historical (c1950) barrier island response with its current (c2000) response to hurricane forcing.

To address the uncertainty in future SLR projections, several scenarios are considered. Scenarios are intended to aid in decision-making when significant uncertainty exists in future outcomes and are important for determining proper adaptation strategies (Moss et al., 2010; Park Science, 2011). In this study, we use projections published by NOAA (Parris et al., 2012) where the highest projections are based on IPCC global SLR projections and include SLR contributions from ice cap melting. Parris et al. (2012) classifies SLR projections as "lowest", "intermediate-low", "intermediate-high" and "highest", corresponding to SLR of +0.2 m, +0.5 m, +1.2 m, and +2.0 m by 2100. Assuming the relative SLR rate for Bay Head (2.4 mm/yr) remains constant over the next century, relative SLR is projected to be as high as +2.2 m by 2100.

By using this method, several assumptions have been made. First, we use the drowned valley or "bathtub" approach (Leatherman, 1990) such that the barrier island has not evolved in response to SLR. As discussed previously, barrier island morphology is sensitive to changes in sea level, becoming unstable and reaching a threshold condition under extreme SLR rates. However, the bathtub method is applicable here because we also assume Bay Head will continue to nourish its beaches to maintain beach widths and dune heights into the future, as it has done for at least the last 50 years. Second, by using SLR scenarios published by Parris et al. (2012), we inherently assume land-ice melting will contribute to rising sea levels, which are not included in scenarios published by Pachauri et al. (2014), for example. Currently, the rate of melting is not known, but it is thought to be the greatest contributor to future SLR (National Research Council, 2012; Overpeck et al., 2006; Rignot et al., 2011). Third, to simplify the analysis, the offshore wave conditions and local surge anomaly of Hurricane Sandy is assumed to remain the same as present day (c2000), regardless of if the storm occurred in the past or future. This enables the use of the validated XBeach model setup for Bay Head during Hurricane Sandy (Smallegan et al., 2016) and the superposition of future sea levels on ocean and bay surge. However, we acknowledge that, as sea levels rise, free surface gradients in surge changes, thereby amplifying or deamplifying bay side storm surge by as much as +/- 15% (Taylor et al., 2015).

4.4.2 Inundation of mean higher high water under sea level rise

In order to visualize the land lost by static impacts of SLR alone, an inundation map using the model grid of the study area is created. The amount of SLR is superimposed onto present-day mean higher high water (MHHW) to determine the future datum position. Elevations that fall below this future MHHW datum are assumed to be inundated during high tide, and inundation extent on the ocean and bay sides for SLR = +1.0 m and +2.2 m are shown in Figure 4.2. Results show relatively minor inundation on the ocean side (right side of grid) but major inundation on the bay side (left side of grid). For SLR of +0.2 m, the beach is inundated by an additional 1 m in the cross-shore direction and an additional 4 m on the bay side in areas that are particularly low-lying. Horizontal inundation distances increase to 7 m on the ocean side and 220 m on the bay side for SLR = +1.0 m. Only the dune ($x = 700$ m) remains above MHHW for extreme SLR (SLR = +2.2 m) and the entire backbarrier region is flooded during high tide. These inundation extents are comparable with those estimated for regional static impacts of SLR by NOAA's National Ocean Service (National Ocean Service, 2015).

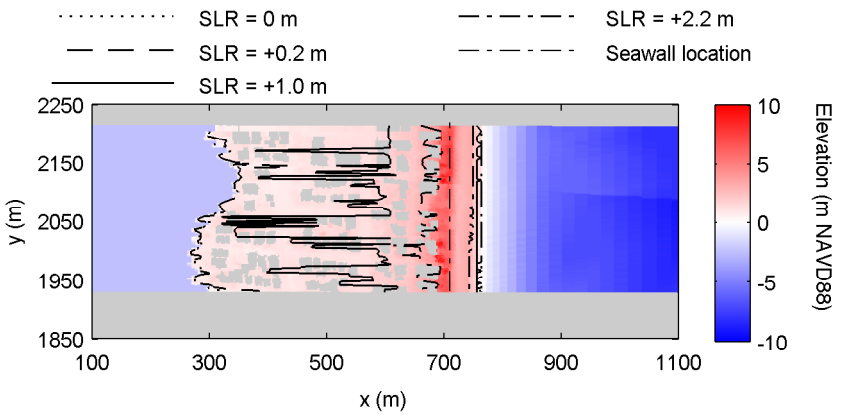

Figure 4.2: Water inundation map of the study area in Bay Head, NJ on the ocean (right) and bay (left) sides under present-day MHHW (dot), SLR = +0.2 m MHHW (dash), SLR = +1.0 m MHHW (solid), and SLR = +2.2 m MHHW (dash-dot). Buildings are represented by gray polygons and the buried seawall is located beneath the dune (vertical dash-dot).

Because coastal storms pose one of the greatest threats to developed barrier islands, it is of interest to analyze its future morphological response to storm surge and waves. XBeach is a wave-group resolving 2DH (two-dimensional horizontal) numerical model originally developed to accurately simulate hydrodynamics and morphology on complex topography during storm events (Roelvink et al., 2009). The process-based model performs with high skill when simulating dune erosion (Van Thiel de Vries, 2009), overwash processes (McCall et al., 2010) and breaching (Roelvink et al., 2009) of sandy beaches. XBeach has also been validated for morphological response of Bay Head to Hurricane Sandy (Figure 4.3). Model performance is determined by comparing post-storm survey data to bed level change simulated with XBeach and calculating the Brier Skill Score (Van Rijn et al., 2003). XBeach performs well with a score of 0.86 where 1.0 indicates perfect model performance (Smallegan et al., 2016). Buildings and the seawall are specified as hard layers in XBeach and are unable to be destroyed by hurricane forcing, as might occur in nature. The reader is referred to Smallegan et al. (2016) for details on the full model setup.

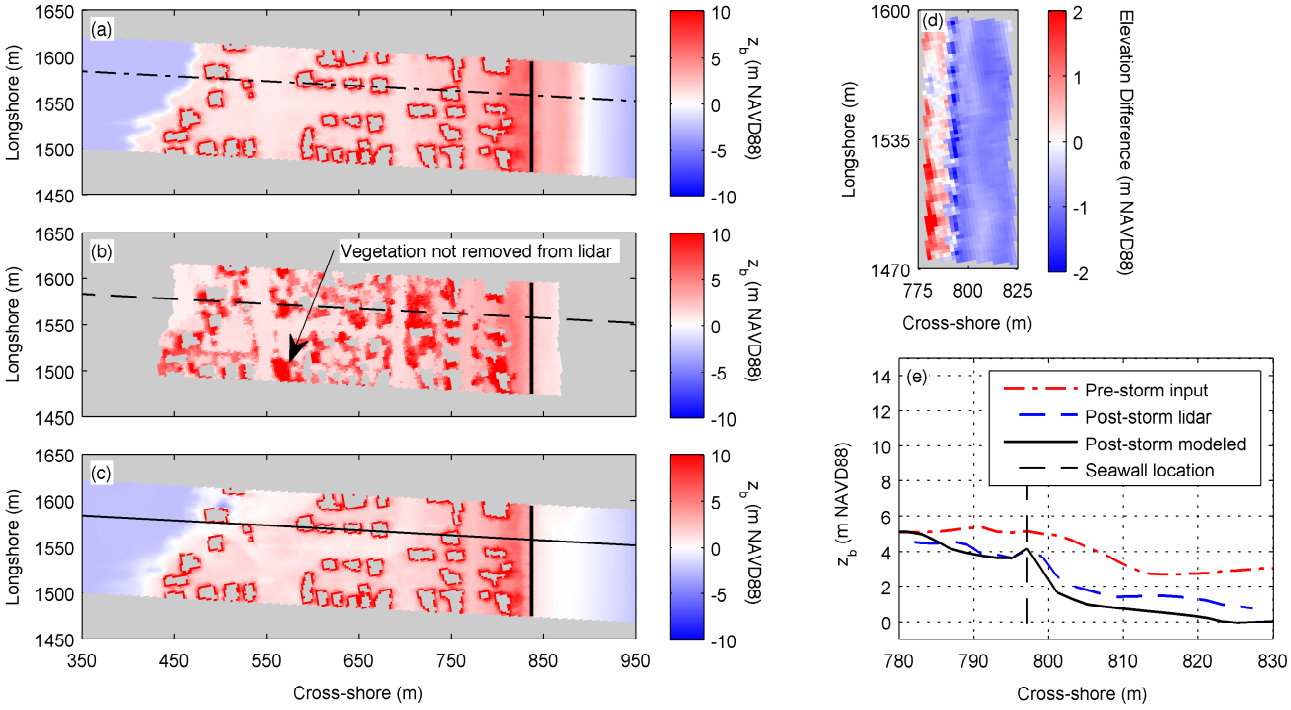

Figure 4.3: Data in the model domain: (a) elevation, z_b, of the pre-storm model input, (b) z_b of the post-storm first return lidar survey where red patches are vegetation that were not removed in the data set, and (c) z_b of the final XBeach result (seawall, black solid line); (d) elevation difference, Δz_b, between the final XBeach result and measured data (XBeach - lidar) for the dune and beach face region; (e) cross-shore profile (dash-dot line in (a), dash line in (b) and solid line in (c)) of pre-storm measurements (dash-dot), post-storm measurements (dash) and final XBeach result (solid). Building locations are shown in gray. Reprinted with permission (see Appendix C) from Smallegan et al. (2016).

Each SLR scenario is superimposed onto the best estimate of storm surge time series for Hurricane Sandy (see Smallegan et al. (2016) for details). Hurricane Sandy (2012) is chosen for this study because of the immense pre- and post- storm data sets available, including high-resolution lidar surveys and in situ measurements of bay surge levels. These data are necessary for accurate model setup and validation. Also, the local bay surge anomaly for this storm is particularly interesting. As the storm passed, bay water levels in Bay Head receded due to southerly winds, but this recession was followed by a sudden increase in surge as wind direction shifted to the north. This anomaly has been observed on uninhabited barrier islands during storms, particularly in the Gulf of Mexico (e.g. Rego and Li, 2010; Sherwood et al., 2014). Because bay surge can affect, or govern in some cases, the morphological change on barrier islands, adaptation strategies to SLR should consider bay surge especially on developed barrier islands.

Morphological change of the island as it exists today is simulated with XBeach. This simple strategy is herein called the Do-Nothing strategy (Figure 4.4) and is intended as a baseline for improvement as adaptation strategies, described in the next section, are implemented. This modeling framework is also applied to evaluate adaptation strategies as discussed below.

4.4.3 Adaptation strategies and performance evaluation

In order for low-lying, developed barrier islands to continue their present-day existence as sea levels rise, adaptation strategies will need to be considered. Here, we perform a sensitivity analysis on the effectiveness of several options listed in Table 4.1 and shown in Figure 4.4. Although we are not optimizing or evaluating all possible combinations of adaptation strategies, we consider strategies currently in practice or those that have been implemented at Bay Head or on other developed barrier islands. XBeach is used to simulate morphological change of each strategy under SLR and hurricane forcing. The total volume of sediment remaining on the island, V, is used as a proxy for damage such that larger V indicates a reduction in damage. Each strategy is compared to the Do-Nothing case. For a given strategy, remaining sediment volume is calculated as

$$V(m^3) = \int_{y_1}^{y_2} \int_{x_1}^{x_2} z_{bf} dx dy \tag{4.1}$$

where z_{bf} is the final simulated topography. Cross-shore locations x_1 and x_2 are used to evaluate the integral for the island, dune and backbarrier regions between longshore locations y_1=1925 m to y_2=2225 m. Additionally, the maximum vertical erosion or scour, $z_{b,min}$, and average final elevation, $z_{b,mean}$, are calculated and used as indicators of reduced scour around structures and overall erosion on the island. In order to estimate the severity of erosion relative to future sea level, these values are shown relative to future MHHW datums, which are assumed to rise by the amount of SLR. Since the buried seawall is a permanent structure currently existing in Bay Head, it is included in all simulations. An analysis of the protection afforded by the seawall compared to its absence is given in Smallegan et al. (2016).

First, we evaluate the island's response to hurricane forcing assuming Bay Head will continue its current practices of routine beach nourishment (Strategy A). Since this area is a popular tourist destination in the U.S. and beach nourishment has been ongoing for at least 50 years, it is very likely that these practices will continue into the future in order to maintain beaches; therefore, it is included in every strategy. Strategy A is implemented by raising the beach by the amount of SLR (i.e. beach is raised 1.0 m for SLR = +1.0 m), where the beach is defined as the region from the toe of the dune to the depth of closure (DOC) (Figure 4.4 (a)). Strategy B combines beach and dune nourishment such that the dune is also raised by the amount of SLR (Figure 4.4 (a)). To maintain beach width and realistic side slopes of the dune, the beach is shifted seaward by up to 4 m. Strategy C combines beach and dune nourishment with raising the elevation of the seawall by 0.5 m, 1.0 m and 2.0 m (Figure 4.4 (b)).

Table 4.1: Strategies considered for adaptation to rising sea levels.

Strategy	Beach raised by SLR amount	Dune raised by SLR amount	Seawall raised by 0.5 m, 1.0 m, 2.0 m	Backbarrier raised to minimum elevation
Do-Nothing				
A	X			
B	X	X		
C	X	X	X	
D	X	X		X
E	X	X	X	X

Strategy D results in raising the grade of the entire island by combining beach and dune nourishment with increasing the elevation of the backbarrier (Figure 4.4 (b)). First, the lowest elevation of the present-day topography relative to MHHW is determined to be 0.2 m above MHHW. Then, as sea levels (and MHHW) rise, locations in the backbarrier region that fall below the 0.2-m lowest elevation with respect to future MHHW are raised to this minimum elevation. Although raising the island is an extreme adaptation strategy, it was implemented in Galveston, TX, USA, a developed barrier island located on the Gulf of Mexico. After narrowly surviving a major hurricane in 1900, which is the greatest U.S. natural disaster in recorded history, the city of Galveston built a 16 km long seawall and raised the island by up to 4 m (Bartee, 2001). Over the last century, Galveston has survived several strong tropical storms, including Hurricane Ike (2008), which destroyed neighboring Bolivar Peninsula (Kennedy et al., 2010; Kraus and Lin, 2009; Williams et al., 2009). Galveston's survival has been largely attributed to the seawall and grade raising (Bartee, 2001). Strategy E combines all adaptation strategies such that the island grade and seawall elevation are both raised (Figure 4.4 (b)).

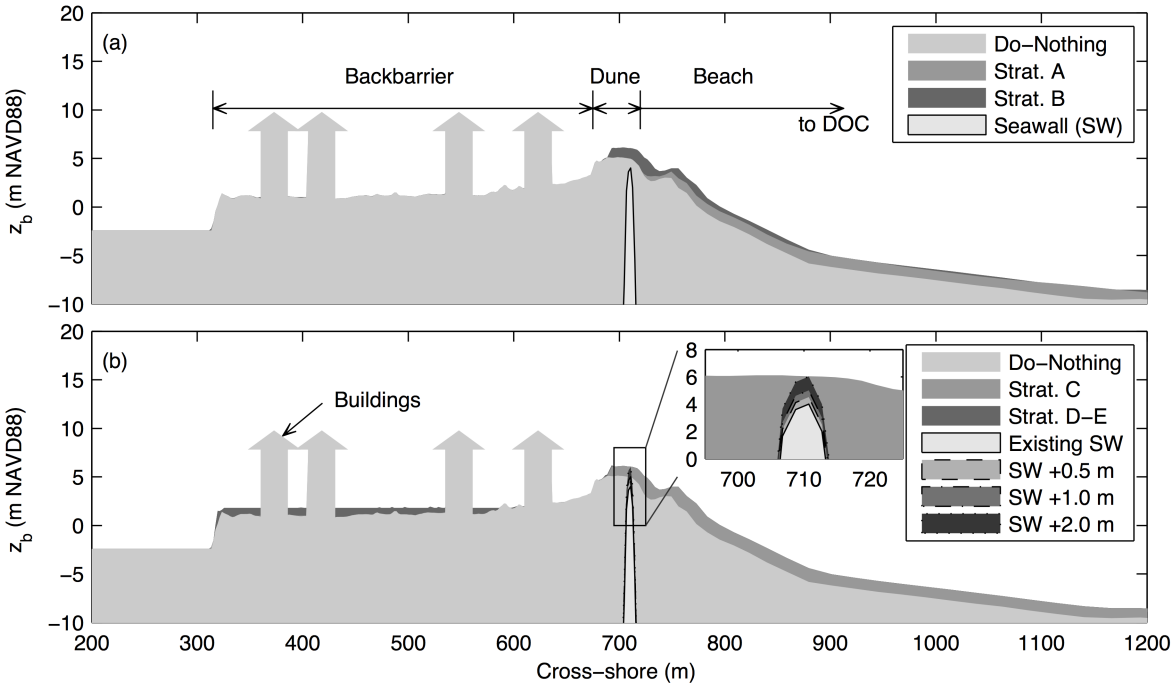

Figure 4.4: A representative cross-shore profile of adaptation strategies as specified in Table 4.1 for SLR = +1.0 m: (a) the Do-Nothing (present-day) elevation (z_b), Strategies A – B and (b) the Do-Nothing (present-day) z_b and Strategies C – E. Buildings are peaks in data and the seawall is represented by shaded regions at cross-shore distance 785 m.

4.5 Results and Discussion

Prior to implementing adaptation strategies, the Do-Nothing case is simulated for SLR scenarios in order to establish a baseline condition of the island's response to hurricane forcing. Figure 4.5 (a) compares cross-shore profiles of the final island topography for past (SLR = -0.2 m), present (SLR = 0 m) and future (SLR = +0.2 m, +1.0 m, and +2.2 m) sea levels. The initial profile is shown for reference. For all SLR scenarios, the berm is severely eroded and sediment is deposited in the nearshore region (Figure 4.5 (a)). The seawall becomes exposed and under extreme SLR, scour holes up to 16 m deep form and the average elevation of the island is below -2 m MHHW (Figure 4.6).

As observed in Figure 4.5, morphological responses are similar between SLR = -0.2 m and 0 m with 560 m^3 and 530 m^3 of sediment remaining on the island. Increasing sea level from

0 m to 0.2 m causes V to decrease by 3%, where the additional sediment loss of 20 m^3 is due to erosion of the dune. As expected, V continues to decrease with SLR as scour holes form behind the seawall and backbarrier elevations are lowered. Nearly the entire sediment volume originating from the island is eroded for SLR = +1.0 m, lowering the overall grade of the island to below 0 m MHHW. For SLR = +2.2 m, erosion exceeds the initial sediment volume by 100 m^3 per unit width. Since more sediment is eroded than initially existing above 0 m NAVD88, the island grade is reduced below this elevation (Figure 4.6 (b)).

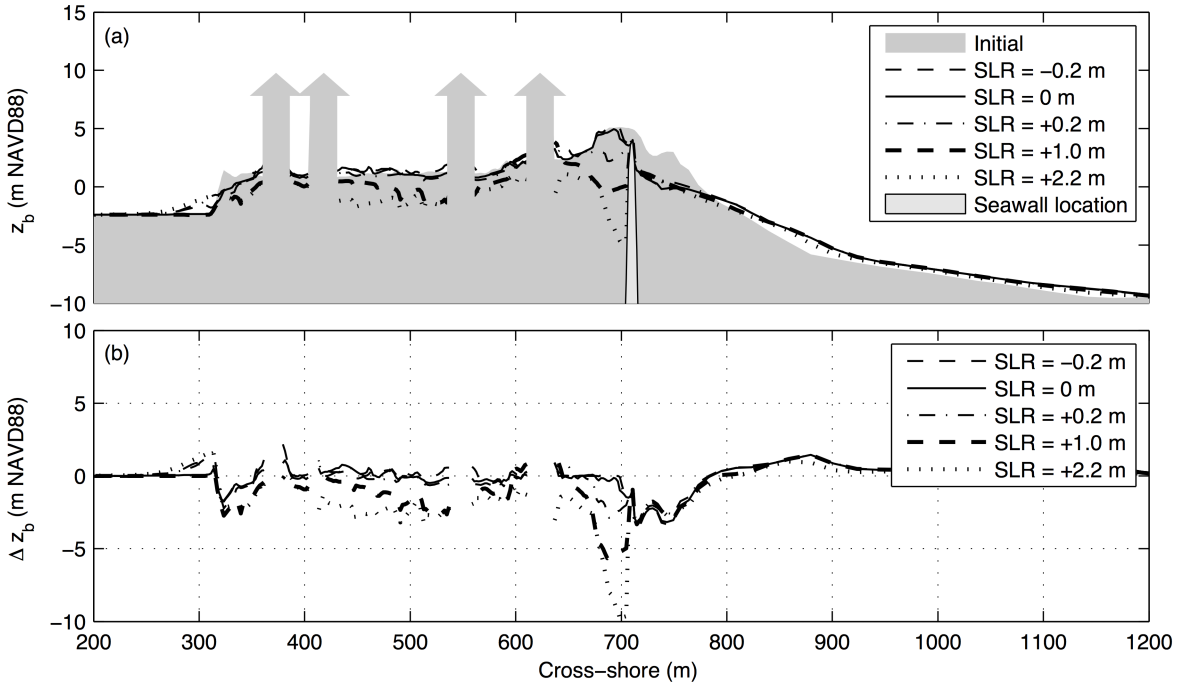

Figure 4.5: Cross-shore profiles through the study area of the Do-Nothing strategy: (a) initial island topography (gray shaded) and final simulated profiles; (b) elevation difference, $\Delta z_b = z_b(final) - z_b(initial)$ for SLR = -0.2 m (dash), SLR = 0 m (solid), SLR = +0.2 m (dash-dot), SLR = +1.0 m (heavy dash) and SLR = +2.2 m (dot); Buildings are peaks in data and the seawall is located along the vertical dash line.

From simulations of the Do-Nothing strategy, two major conclusions are drawn. First, in the past, the island did not experienced significant increases in storm-induced erosion as sea levels rose, and the dune system remained relatively in tact. However, a small rise in sea level (+0.2 m) above the present-day condition causes significant erosion on the dune. According to Parris et al. (2012) and Pachauri et al. (2014), a 0.2 m rise in sea level is likely to occur by the mid to late 21st century even in the most conservative projections. Secondly, extreme SLR causes V to decrease, but the backbarrier elevation is particularly impacted and is reduced to elevations below 0 m below present-day NAVD88 (3 m below future MHHW). Clearly, this would cause catastrophic damage to infrastructure and threatens the viability

of the barrier island system. Most coastal structures are placed on the beach to protect the island from ocean side processes (National Research Council, 2014), but our results suggest the backbarrier is particularly vulnerable under future SLR.

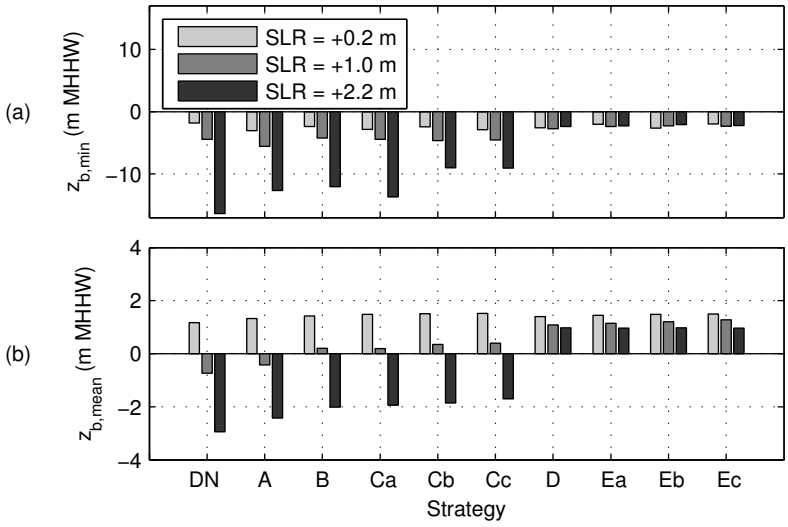

Figure 4.6: Simulated minimum, $z_{b,min}$ (a) and average, $z_{b,mean}$ (b) island elevations relative to future MHHW datums as sea levels rise for each strategy and SLR scenario. DN represents the Do-Nothing strategy, Ca and Ea represent Strategies C and E for seawall raised 0.5 m, Cb and Eb represent Strategies C and E for seawall raised 1 m, and Cc and Ec represent Strategies C and E for seawall raised 2 m.

Using the Do-Nothing strategy as a baseline for improvement, adaptation Strategies A – E are implemented for SLR = +0.2 m, +1.0 m and +2.2 m. In addition to calculating minimum and mean final island elevations relative to future MHHW (Figure 4.6), Equation 4.1 is used to calculate sediment volumes remaining on the island, dune and backbarrier after the storm (Figure 4.7). From simulations of Strategy A and SLR scenarios, XBeach predicts the additional sediment placed on the beach is transported offshore during the storm. Scour and erosion on the island are not significantly reduced for SLR = +0.2 m and +1.0 m, with minimum and mean elevations varying by +/- 1 m from the Do-Nothing case. For SLR = +0.2 m, scour holes behind the seawall are deeper than those formed for the Do-Nothing strategy due to longshore variability in the eroded beach. In the dune region for SLR = +1.0 m and +2.2 m, V_{dune} increases from 100 m^3 and 10 m^3 to 165 m^3 and 140 m^3 (Figure 4.7 (b)), but dune heights are severely reduced and the remaining sediment volume is due to filling of the scour holes behind the seawall by overwashed dune sediment. Under extreme SLR, the minimum elevation is reduced from -13 m to -10 m and the average elevation of the island becomes positive (Figure 4.6), but $V_{backbarrier}$ remains negative and at critically low elevations (Figure 4.7 (c)).

Compared to the Do-Nothing case, Strategies B and C show reductions in scour depths and increases in average elevations of less than 1 m for SLR = +0.2 m and +1.0 m (Figure 4.6). For SLR = +2.2 m, raising the seawall by 1 m or 2 m reduces minimum elevation by 7 m and increases average island elevation by 1 m, resulting in slight increases in V_{island} (Figure 4.6). This is due to more sediment remaining on the dune (V_{dune} increases from the Do-Nothing case) since $V_{backbarrier}$ decreases when dune or seawall height increases. As dune heights are increased in Strategies B and C, the backbarrier is flooded and severely eroded when bay surge levels rise since the dunes can no longer be inundated. For the Do-Nothing strategy, dune heights are reduced during the peak of the storm due to inundation by ocean surge, allowing bay side surge to flow freely over the island.

From Figures 4.6–4.7, Strategies D and E are the most effective at decreasing scour depths and increasing V, thus, protecting the barrier island from hurricane forcing under SLR. Minimum final elevations remain nearly the same for SLR = +0.2 m, but increase by at least 1.7 m for SLR = +1.0 m, and increase by at least 14 m for SLR = +2.2 m compared to the Do-Nothing case. Average island elevations increase in all scenarios for Strategies D and E, where $z_{b,mean}$ is 0.3 m, 2 m, and 4 m higher compared to the Do-Nothing case for SLR = +0.2 m, +1.0 m, and +2.2 m. These results indicate raising the island protects the island from hurricane forcing, especially as SLR reaches extreme levels.

Analyzing V on the island, dune and backbarrier for these strategies and SLR scenarios, it is obvious V_{island} for moderate to extreme SLR increases compared to the Do-Nothing case due to increases in $V_{backbarrier}$ (i.e. V_{dune} remains nearly the same). Since the backbarrier region was not greatly affected by SLR = +0.2 m, V remains nearly unchanged for Strategies D and E. Also, for Strategies Do-Nothing, A, B, and C, V decreases as SLR increases. However, for Strategies D and E, this relationship becomes direct since more sediment is added to the island prior to the storm but is not transported during the simulation. Therefore, raising the island prevents its overall elevation from being eroded to critically low elevations, particularly on the backbarrier.

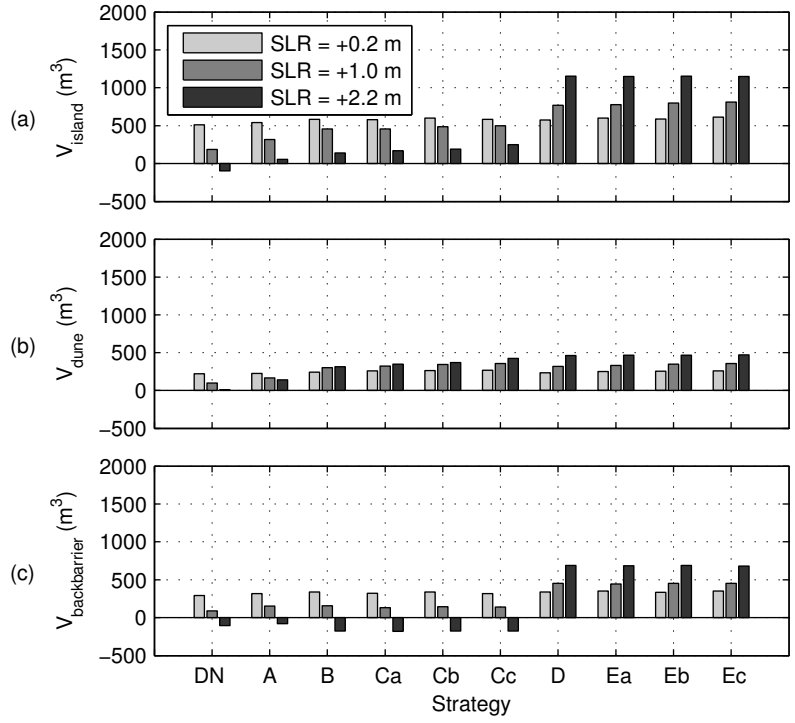

Figure 4.7: V for the (a) island (x_1 = 300 m, x_2 = 770 m), (b) dune (x_1 = 650 m, x_2 = 770 m), and (c) backbarrier (x_1 = 300 m, x_2 = 650 m) for each strategy and SLR scenario. DN represents the Do-Nothing strategy, Ca and Ea represent Strategies C and E for seawall raised 0.5 m, Cb and Eb represent Strategies C and E for seawall raised 1 m, and Cc and Ec represent Strategies C and E for seawall raised 2 m.

In general, results show the sediment volume remaining on the island is independent on seawall height for any SLR scenario. Because seawalls are capable of protecting barrier island during storm events (Bartee, 2001; Irish et al., 2013; Smallegan et al., 2016), it is expected that seawalls will become increasingly important for protecting developed barrier islands as sea levels rise (National Research Council, 2014). However, results shown in Figure 4.7 indicate increasing seawall height up to 2 m does not cause V to increase, i.e. V_{island} is nearly the same between Strategies Ca, Cb and Cc and between Strategies Ea, Eb, and Ec. Therefore, once the seawall exceeds some minimum threshold elevation (dependent on several island and storm characteristics including island location and storm intensity), the protection afforded the island by the seawall does not increase with peak seawall height.

4.6 Conclusions

In this study, ten adaptation strategies have been evaluated on their effectiveness at reducing damage on a low-lying developed barrier island under three future SLR scenarios. Using a numerical model to simulate hydrodynamics and morphological change, results show Strategy A (beach raised) to offer only slight protection for the barrier island as sea levels rise. For minor to moderate SLR, Strategies B (raised beach and dune) and C (raised beach, dune and seawall) are viable options for protecting the barrier island from hurricane forcing, but as sea levels rise to extreme levels, raising dune heights and seawall elevations exacerbate erosion in the backbarrier region. Strategy B, which is a commonly used nature-based adaptation strategy especially in the U.S. since the 1970s (Cunniff and Schwartz, 2015; National Research Council, 2014), offers additional protection to the island over the Do-Nothing strategy for "intermediate-high" SLR. In general, raising the seawall (Strategies C and E) reduces volumetric erosion on the dune compared to the Do-Nothing strategy for all SLR scenarios considered here. However, raising the seawall is typically more expensive and invasive than beach nourishment as an adaptation measure. Of the adaptation strategies considered, land reclamation (i.e. Strategies D and E) is the only option that offers a significant reduction in dune and backbarrier erosion over the Do-Nothing strategy. Although it is an extensive and invasive adaptation strategy, raising island elevation provides both short-term (i.e. minor SLR) as well as long-term (i.e. extreme SLR) protection according to the results of this study.

In future work, the limitations of this study should be minimized by expanding simulations to other developed barrier islands under different storm forcing. Since shorelines change in response to SLR, a new equilibrium profile should be estimated prior to implementing adaptation strategies. As sea levels rise, the effectiveness of these strategies should be re-evaluated and the vulnerability of the backbarrier region reassessed in order to prevent exacerbating backbarrier erosion due to bay side inundation during storms. Also, a life cycle cost analysis should be performed on each strategy to determine the most feasible alternatives as sea level rises. For example, over time and as sea levels continue to rise, the cost of periodic renourishment may be greater than the initial construction costs of raising the island. In the future, coastal planners will need to consider protection from bay side flooding, as well as ocean surge and waves on low-lying barrier islands.

Acknowledgments

This material is based upon work supported by the National Oceanic and Atmospheric Administration, U.S. Department of Commerce, via award number NA14OAR4170093 to Virginia Sea Grant; the National Science Foundation Graduate Research Fellowship Program via grant number DGE-1148903; and National Science Foundation via grant number EAR-1312813. A. Van Dongeren was supported through Deltares Research Program on "Hydro-

and Morphodynamics during Extreme Events". The authors acknowledge Advanced Research Computing at Virginia Tech for providing computational resources and technical support that have contributed to the results reported within this paper, http://www.arc.vt.edu.

Chapter 5

Conclusions

In this dissertation, the morphological change of a developed barrier island to Hurricane Sandy (2012) forcing is simulated using a numerical model. The study area, Bay Head, NJ, USA is fronted with a buried rock seawall and backed by long, narrow Barnegat Bay. Simulations from the morphological model, XBeach, are used to evaluate the effectiveness of the seawall at blocking damaging wave attack on the island, the resulting morphological change due to elevated bay side surge levels, and the protection afforded the island by adaptation strategies to sea level rise. XBeach is a process-based model designed to analyze the effects of ocean and bay side hydrodynamics on morphological changes of complex topography, such as barrier islands. Overall, the main conclusions of this work are:

- A buried rock seawall effectively reduced wave forces on a developed barrier island by a factor of 1.7 compared to locations without a seawall, preserving the dune system and preventing severe erosion due to bay side flooding (Chapter 2).
- Increasing bay surge magnitude or shifting the occurrence of peak bay surge such that it occurs after peak ocean surge exacerbates erosion on the barrier island in the absence of a seawall (Chapter 3).
- Raising elevations of the dune and beach are effective adaptation strategies to moderate sea level rise, but raising island elevations is the only option considered that protects the island from severe morphological change under extreme sea level rise (Chapter 4).

Results presented in Chapter 2 show the validation of the XBeach model setup for Hurricane Sandy as it impacted Bay Head and the morphological change in the presence and absence of a seawall. Neighboring Bay Head on its southern side, the borough of Mantoloking had similar characteristics to Bay Head prior to Hurricane Sandy's landfall, including infrastructure development, island width and dune heights. However, severe dune overwash and two major breaches occurred in Mantoloking, which is not fronted with a buried seawall. Using the validated XBeach setup to compare morphological changes to the island in the presence

and absence of the seawall, it is concluded the seawall in Bay Head protected the island by blocking wave energy during the peak of the storm. In the absence of the seawall, scour holes formed at oceanfront buildings and flow channelization between buildings caused severe erosion on the island. However, the largest volumes of sediment transported corresponded to a sudden increase in bay surge. In the presence of the seawall, the seawall blocked ocean surge and waves from destroying the dune system, which in turn prevented bay surge from inundating the island and causing catastrophic erosion.

In Chapter 3, the timing and magnitude of bay surge as measured during Hurricane Sandy is altered to analyze the effect of bay surge on morphological change. The same model setup validated in Chapter 2 is used, and volumetric bed level change is used as a proxy for damage (i.e. when V_C is greater than V_{NC}, damage is increased under the new condition, C, compared to the No Change condition, NC). For the alterations to bay surge considered here, damage is expected to exceed damage observed during Hurricane Sandy conditions only when bay surge magnitude increases. All other alterations indicate a reduction in damage both in the presence and absence of a seawall. Damage is greatly reduced when peak bay surge corresponds to or occurs prior to peak ocean surge. Therefore, the impact of Hurricane Sandy on Mantoloking was overly devastating due to the timing and magnitude of bay surge relative to ocean surge. As observed in Chapter 2, results in Chapter 3 show the seawall protected Bay Head from catastrophic damages by reducing both ocean and bay side impacts, even though it is designed to protect only against ocean forcing.

In addition to the seawall's effectiveness in reducing Hurricane Sandy impacts, several adaptation strategies to three SLR scenarios are evaluated in Chapter 4. Again, morphological change is simulated for the validated model setup, where varying sea levels (-0.2 m, 0 m, +0.2 m, +1.0 m, and +2.2 m) are superimposed on ocean and bay surge levels. XBeach results show, for past sea level (-0.2 m corresponding to c1950 sea level), bed level changes in Bay Head are relatively small; but, for future sea level (+0.2 m), dune heights are lowered by 2 m. As sea levels rise, V, or the volume of sediment remaining on the island after the simulated storm, decreases, indicating an increase in damage. For future SLR and Strategies A - C, minimum elevations (i.e. scour around structures) generally decrease and average island elevations increase compared to the Do-Nothing strategy. However, backbarrier elevations are reduced to critical levels under extreme SLR, and Strategies A - C do not offer any additional protection to the backbarrier for any SLR scenario. Only raising island grade protects the island from bay side inundation under all sea level rise scenarios. As sea levels rise, the effectiveness of raising the island to protect it from catastrophic erosion increases.

Although results from this study show the seawall is effective at protecting a developed barrier island from hurricane forcing, the results should not be overextended to apply to all barrier islands or storm conditions. First, this work is specific to a single study location and storm; therefore, the results are only applicable in study locations with similar topography and for storms with similar forcing. Second, the seawall simulated here is a sloping structure buried beneath nourished dunes. Other types of seawalls, such as vertical sheet-pile walls or exposed concrete structures, reflect wave energy, which will cause the morphological change

to vary from the results shown here. Thirdly, daily wind and wave conditions near Bay Head cause the seawall to remain covered until a strong wave or swell event occurs. If improperly designed, the seawall can exacerbate erosion on sandy beaches, especially those that are eroding or require periodic renourishment. Each of these considerations must be taken into account when analyzing the results presented herein.

In future work, the effect of buildings on the morphological change of the island should be analyzed. It is hypothesized that the buildings, which are indestructible in XBeach, cause channelization of flow during the inundation regime, increasing erosion between the buildings. Similarly, vegetation cover should be included in future numerical analysis to determine the extent to which vegetation dissipates wave energy and reduces erosion as the island is inundated. Since Bay Head has small dense patches of vegetation as opposed to uniformly distributed vegetation, its effect on morphological change should be analyzed and quantified.

Additionally, the model area should be extended into the bay in order to determine the effects of bay bathymetry on barrier island breaching. For example, in Barnegat Bay, a channel having greater depths than most of the bay is observed to meander, becoming close to the bay side of Mantoloking. At that location, a breach forms through the island. Future work should investigate this process and the effect of bay bathymetry on barrier island morphological response to hurricane forcing.

As mentioned in Chapter 4, a cost-benefit analysis in terms of amount of SLR should be performed on each adaptation strategy. The cost of strategy implementation is a function of SLR, the amount of time required to reach that sea level, and the compounding cost of beach fill and periodic renourishment. Therefore, the benefit of implementing a given strategy will, in turn, depend on amount of SLR and project longevity as it is impacted by storms. A simple tool estimating the cost of each strategy per increase in sea level would be useful to coastal planners as management plans are designed for protecting barrier islands.

Bibliography

Ablain, M., Cazenave, A., Valladeau, G., and Guinehut, S. (2009). A new assessment of the error budget of global mean sea level rate estimated by satellite altimetry over 1993-2008. *Ocean Science*, 5(2):193–201.

Associated Press (2015). New Jersey shore eroded after storm. *The Wall Street Journal*. http://www.wsj.com/articles/new-jersey-shore-eroded-after-storm-1444088546, Accessed 9 February 2016.

Bartee, C. (2001). Galveston Seawall and Grade Raising Project Located on the Gulf of Mexico, Galveston Island, Texas. In *International Engineering History and Heritage@ sImproving Bridges to ASCEs 150th Anniversary*, pages 461–469. ASCE.

Basco, D. R. (1998). The economic analysis of "soft" versus "hard" solutions for shore protection: An example. *Coastal Engineering Proceedings*, 1(26).

Basco, D. R. (2000). Beach monitoring results and management plan FCTCLANT, Dam Neck, Virginia Beach, VA. Technical report, Beach Consultants, Inc.

Blake, E. S., Kimberlain, T. B., Berg, R. J., Cangialosi, J., and Beven II, J. L. (2013). Tropical cyclone report: Hurricane Sandy. *National Hurricane Center*, 12:1–10.

Booij, N., Ris, R., and Holthuijsen, L. H. (1999). A third-generation wave model for coastal regions: 1. Model description and validation. *Journal of Geophysical Research: Oceans (1978–2012)*, 104(C4):7649–7666.

Church, J. A. and White, N. J. (2011). Sea-level rise from the late 19th to the early 21st century. *Surveys in Geophysics*, 32(4-5):585–602.

Claudino-Sales, V., Wang, P., and Horwitz, M. H. (2008). Factors controlling the survival of coastal dunes during multiple hurricane impacts in 2004 and 2005: Santa Rosa barrier island, Florida. *Geomorphology*, 95(3):295–315.

Crossett, K., Ache, B., Pacheco, P., and Haber, K. (2013). National coastal population report: Population trends from 1970 - 2010. Technical report, National Oceanic and Atmospheric Administration.

Crowell, M., Coulton, K., Johnson, C., Westcott, J., Bellomo, D., Edelman, S., and Hirsch, E. (2010). An estimate of the us population living in 100-year coastal flood hazard areas. *Journal of Coastal Research*, pages 201–211.

Cunniff, S. and Schwartz, A. (2015). Performance of natural infrastructure and nature-based measures as coastal risk reduction features. *Envionmental Defense Fund*.

Dean, R. G. and Dalrymple, R. A. (2004). *Coastal processes with engineering applications*. Cambridge University Press.

Dennison, W. C., Saxby, T., and Walsh, B. M. (2012). Responding to major storm impacts: Chesapeake Bay and the Delmarva Coastal Bays.

Department of Environmental Protection (1999). Geologic Map of New Jersey. Technical report, Division of Science, Research and Technology Geological Survey.

Donnelly, C., Kraus, N., and Larson, M. (2006). State of knowledge on measurement and modeling of coastal overwash. *Journal of Coastal Research*, pages 965–991.

Escudero, M., Mendoza, E., Silva-Casarín, R., and Villatoro, M. (2014). Comparative risk assessment at Isla del Carmen and Cancun, Mexico. *Coastal Engineering Proceedings*, 1(34):10.

Escudero Castillo, M., Mendoza Baldwin, E., Silva Casarin, R., Posada Vanegas, G., and Arganis Juaréz, M. (2012). Characterization of risks in coastal zones: A review. *CLEAN–Soil, Air, Water*, 40(9):894–905.

Feagin, R. A., Figlus, J., Zinnert, J. C., Sigren, J., Martínez, M. L., Silva, R., Smith, W. K., Cox, D., Young, D. R., and Carter, G. (2015). Going with the flow or against the grain? The promise of vegetation for protecting beaches, dunes, and barrier islands from erosion. *Frontiers in Ecology and the Environment*, 13(4):203–210.

Gibeaut, J. C., Hepner, T. L., Waldinger, R., Andrews, J. R., Smyth, R. C., and Gutierrez, R. (2003). Geotubes for temporary erosion control and storm surge protection along the Gulf of Mexico shoreline of Texas. *Proceedings of the 13th Biennial Coastal Zone Conference*, 13:17.

Goff, J. A., Allison, M. A., and Gulick, S. P. (2010). Offshore transport of sediment during cyclonic storms: Hurricane Ike (2008), Texas Gulf Coast, USA. *Geology*, 38(4):351–354.

Google, Inc. (2014). Google Earth version 7.1. http://www.google.com /earth/index.html, Accessed 12 April 2013.

Gutierrez, B. T., Williams, S. J., and Thieler, E. R. (2007). Potential for shoreline changes due to sea-level rise along the us mid-atlantic region. Technical report.

Halverson, J. B. and Rabenhorst, T. (2013). Hurricane Sandy: The science and impacts of a superstorm. *Weatherwise*, 66(2):14–23.

Hinrichsen, D. (1999). *Coastal waters of the world: Trends, threats, and strategies*. Island Press.

Houser, C., Hapke, C., and Hamilton, S. (2008). Controls on coastal dune morphology, shoreline erosion and barrier island response to extreme storms. *Geomorphology*, 100(3):223–240.

Irish, J. L., Lynett, P. J., Weiss, R., Smallegan, S. M., and Cheng, W. (2013). Buried relic seawall mitigates Hurricane Sandy's impacts. *Coastal Engineering*, 80:79–82.

Jevrejeva, S., Moore, J., Grinsted, A., and Woodworth, P. (2008). Recent global sea level acceleration started over 200 years ago? *Geophysical Research Letters*, 35(8).

Kennedy, A., Rogers, S., Sallenger, A., Gravois, U., Zachry, B., Dosa, M., and Zarama, F. (2010). Building destruction from waves and surge on the Bolivar Peninsula during Hurricane Ike. *Journal of Waterway, Port, Coastal, and Ocean Engineering*, 137(3):132–141.

Kraus, N. C. and Lin, L. (2009). Hurricane Ike along the upper Texas Coast: an introduction. Technical report, DTIC Document.

Kraus, N. C. and McDougal, W. G. (1996). The effects of seawalls on the beach: Part I, an updated literature review. *Journal of Coastal Research*, pages 691–701.

Kraus, N. C. and Wamsley, T. V. (2003). Coastal Barrier Breaching. Part 1. Overview of Breaching Processes. Technical report, DTIC Document.

Leatherman, S. P. (1990). Modelling shore response to sea-level rise on sedimentary coasts. *Progress in Physical Geography*, 14(4):447–464.

Lennon, G. (1991). The nature and causes of hurricane-induced ebb scour channels on a developed shoreline. *Journal of Coastal Research*, pages 237–248.

Lindemer, C., Plant, N., Puleo, J., Thompson, D., and Wamsley, T. (2010). Numerical simulation of a low-lying barrier island's morphological response to Hurricane Katrina. *Coastal Engineering*, 57(11):985–995.

Lowe, S. R., Sampson, L., Gruebner, O., and Galea, S. (2015). Psychological resilience after Hurricane Sandy: The influence of individual-and community-level factors on mental health after a large-scale natural disaster. *PloS one*, page e0125761.

McCall, R., De Vries, J. V. T., Plant, N., Van Dongeren, A., Roelvink, J., Thompson, D., and Reniers, A. (2010). Two-dimensional time dependent hurricane overwash and erosion modeling at Santa Rosa Island. *Coastal Engineering*, 57(7):668–683.

McGranahan, G., Balk, D., and Anderson, B. (2007). The rising tide: Assessing the risks of climate change and human settlements in low elevation coastal zones. *Environment and urbanization*, 19(1):17–37.

McKay, N. P., Overpeck, J. T., and Otto-Bliesner, B. L. (2011). The role of ocean thermal expansion in last interglacial sea level rise. *Geophysical Research Letters*, 38(14).

Morton, R. A. (1976). Effects of Hurricane Eloise on beach and coastal structures, Florida Panhandle. *Geology*, 4(5):277–280.

Morton, R. A. (2002). Factors controlling storm impacts on coastal barriers and beaches: a preliminary basis for near real-time forecasting. *Journal of Coastal Research*, pages 486–501.

Moss, R. H., Edmonds, J. A., Hibbard, K. A., Manning, M. R., Rose, S. K., Van Vuuren, D. P., Carter, T. R., Emori, S., Kainuma, M., Kram, T., et al. (2010). The next generation of scenarios for climate change research and assessment. *Nature*, 463(7282):747–756.

Mulshine, P. (2015). *That steel wall on the beach is turning out to be a disaster for public access.* New Jersey Online. http://www.nj.com/opinion/index.ssf/2015/10/jerseyfication_rocks.html, Accessed 9 February 2016.

National Data Buoy Center (2012). *Station 44025 (LLNR 830) - Long Island - 30 NM South of Islip, NY.* National Oceanic and Atmospheric Administration. http://www.ndbc.noaa.gov/station_page.php?station=44025, Accessed 26 September 2014.

National Geophysical Data Center (2013). *National Geophysical Data Center, U.S. Coastal Relief Model.* National Oceanic and Atmospheric Administration. http://www.ngdc.noaa.gov/mgg/coastal/crm.html, Accessed 21 August 2013.

National Ocean Service (2015). Sea level rise and coastal flooding impacts. National Oceanic and Atmospheric Administration, https://coast.noaa.gov/slr/. Accessed 29 December 2015.

National Research Council (2012). *Sea-Level Rise for the Coasts of California, Oregon, and Washington:: Past, Present, and Future.* National Academies Press.

National Research Council (2014). *Reducing coastal risk on the East and Gulf Coasts.* National Academies Press.

Nederhoff, C. (2014). Modeling the effects of hard structures on dune erosion and overwash: Hindcasting the impact of Hurricane Sandy on New Jersey with XBeach. Master's thesis, Delft University of Technology.

Neumann, B., Vafeidis, A. T., Zimmermann, J., and Nicholls, R. J. (2015). Future coastal population growth and exposure to sea-level rise and coastal flooding–a global assessment. *PloS one*, 10(3):e0118571.

Nicholls, R. J. and Cazenave, A. (2010). Sea-level rise and its impact on coastal zones. *Science*, 328(5985):1517–1520.

NOAA Tides and Currents (2015). *NOAA Tides and Currents*. National Oceanic and Atmospheric Administration. http://tidesandcurrents.noaa.gov/, Accessed 2 February 2016.

Orton, P., Georgas, N., Blumberg, A., and Pullen, J. (2012). Detailed modeling of recent severe storm tides in estuaries of the New York City region. *Journal of Geophysical Research: Oceans (1978–2012)*, 117(C9).

Overpeck, J. T., Otto-Bliesner, B. L., Miller, G. H., Muhs, D. R., Alley, R. B., and Kiehl, J. T. (2006). Paleoclimatic evidence for future ice-sheet instability and rapid sea-level rise. *Science*, 311(5768):1747–1750.

Pachauri, R. K., Allen, M., Barros, V., Broome, J., Cramer, W., Christ, R., Church, J., Clarke, L., Dahe, Q., Dasgupta, P., et al. (2014). Climate Change 2014: Synthesis Report. Contribution of Working Groups I, II and III to the Fifth Assessment Report of the Intergovernmental Panel on Climate Change.

Park Science (2011). Special issue: Climate change adaptation & communication. Technical Report 28:1, National Park Service, U.S. Department of the Interior.

Parris, A., Bromirski, P., Burkett, V., Cayan, D. R., Culver, M., Hall, J., Horton, R., Knuuti, K., Moss, R., Obeysekera, J., et al. (2012). *Global sea level rise scenarios for the United States National Climate Assessment*. US Department of Commerce, National Oceanic and Atmospheric Administration, Oceanic and Atmospheric Research, Climate Program Office.

Peduzzi, P., Chatenoux, B., Dao, H., De Bono, A., Herold, C., Kossin, J., Mouton, F., and Nordbeck, O. (2012). Global trends in tropical cyclone risk. *Nature climate change*, 2(4):289–294.

Pilkey, O. H. and Wright III, H. L. (1988). Seawalls versus beaches. *Journal of Coastal Research*, pages 41–64.

Plant, N. G. and Stockdon, H. F. (2012). Probabilistic prediction of barrier-island response to hurricanes. *Journal of Geophysical Research: Earth Surface*, 117(F3).

Rego, J. L. and Li, C. (2010). Storm surge propagation in Galveston Bay during Hurricane Ike. *Journal of Marine Systems*, 82(4):265–279.

Remington & Boyd Engineers (1962). Construction plans: Stone seawall and groins, Borough of Bay Head, Ocean County, New Jersey. Technical Report Project number 9:02-420-401-881, Department of Conservation and Economic Development.

Rignot, E., Velicogna, I., Van den Broeke, M., Monaghan, A., and Lenaerts, J. (2011). Acceleration of the contribution of the Greenland and Antarctic ice sheets to sea level rise. *Geophysical Research Letters*, 38(5).

Roelvink, D., Reniers, A., Van Dongeren, A., de Vries, J. V. T., McCall, R., and Lescinski, J. (2009). Modelling storm impacts on beaches, dunes and barrier islands. *Coastal Engineering*, 56(11):1133–1152.

Sallenger, A. H. (2000). Storm impact scale for barrier islands. *Journal of Coastal Research*, pages 890–895.

Sallenger Jr, A. H., Doran, K. S., and Howd, P. A. (2012). Hotspot of accelerated sea-level rise on the Atlantic coast of North America. *Nature Climate Change*, 2(12):884–888.

Salter, E. (2007). *Salter's History of Monmouth and Ocean Counties New Jersey: Embracing A Geneological Record of Earliest Settlers in Monmouth and Ocean Counties and their Descendants (originally published in 1890).* Heritage Books Inc., Westminster, MD.

Sheng, Y. P., Zhang, Y., and Paramygin, V. A. (2010). Simulation of storm surge, wave, and coastal inundation in the Northeastern Gulf of Mexico region during Hurricane Ivan in 2004. *Ocean Modelling*, 35(4):314–331.

Sherwood, C. R., Long, J. W., Dickhudt, P. J., Dalyander, P. S., Thompson, D. M., and Plant, N. G. (2014). Inundation of a barrier island (Chandeleur Islands, Louisiana, USA) during a hurricane: Observed water-level gradients and modeled seaward sand transport. *Journal of Geophysical Research: Earth Surface*, 119(7):1498–1515.

Silva, R., Martínez, M. L., Hesp, P. A., Catalan, P., Osorio, A. F., Martell, R., Fossati, M., Miot da Silva, G., Mariño-Tapia, I., Pereira, P., et al. (2014). Present and future challenges of coastal erosion in Latin America. *Journal of Coastal Research*, 71(sp1):1–16.

Small, C. and Nicholls, R. J. (2003). A global analysis of human settlement in coastal zones. *Journal of Coastal Research*, pages 584–599.

Smallegan, S. M., Irish, J. L., Van Dongeren, A. R., and Den Bieman, J. P. (2016). Morphological response of a sandy barrier island with a buried seawall during Hurricane Sandy. *Coastal Engineering*, 110:102–110.

Smith, A., Lott, N., Houston, T., Shein, K., and Crouch, J. (2015). Billion-Dollar U.S. Weather and Climate Disasters 1980 - 2014. Technical report, National Oceanic and Atmospheric Administration.

Smith, A. B. and Katz, R. W. (2013). U.S. billion-dollar weather and climate disasters: data sources, trends, accuracy and biases. *Natural Hazards*, 67(2):387–410.

Sorensen, R. M. (2005). *Basic Coastal Engineering*, volume 10. Springer Science & Business Media.

Stutz, M. L. and Pilkey, O. H. (2001). A review of global barrier island distribution. *Journal of Coastal Research*, pages 15–22.

Subaiya, S., Moussavi, C., Velasquez, A., and Stillman, J. (2014). A rapid needs assessment of the Rockaway Peninsula in New York City after Hurricane Sandy and the relationship of socioeconomic status to recovery. *American Journal of Public Health*, 104(4):632–638.

Sun, H., Grandstaff, D., and Shagam, R. (1999). Land subsidence due to groundwater withdrawal: potential damage of subsidence and sea level rise in southern New Jersey, USA. *Environmental Geology*, 37(4):290–296.

Taylor, N. R., Irish, J. L., Udoh, I. E., Bilskie, M. V., and Hagen, S. C. (2015). Development and uncertainty quantification of hurricane surge response functions for hazard assessment in coastal bays. *Natural Hazards*, 77(2):1103–1123.

The Richard Stockton Coastal Research Center [RSCRC] (2012). Beach-dune performance assessment of New Jersey Beach Profile Network (njbpn) sites at Northern Ocean County, New Jersey after Hurricane Sandy related to FEMA disaster DR-NJ 4086. Technical report, The Richard Stockton College of New Jersey, Pomona, NJ.

The Richard Stockton Coastal Research Center [RSCRC] (2015). *New Jersey Coastal Composition*. http://intraweb.stockton.edu/eyos/page.cfm?siteID=149&pageID=3.

Thieler, E. R. and Young, R. S. (1991). Quantitative evaluation of coastal geomorphological changes in South Carolina after Hurricane Hugo. *Journal of Coastal Research*, pages 187–200.

Titus, J. G. and Anderson, K. E. (2009). *Coastal sensitivity to sea-level rise: a focus on the mid-Atlantic region*, volume 4. Government Printing Office.

U.S. Army Corps of Engineers (2010). 2010 USACE lidar: New Jersey. http://www.csc.noaa.gov/digitalcoast/data/coastallidar/download, Accessed 31 July 2013.

U.S. Army Corps of Engineers [USACE] (2008). Coastal Engineering Manual, Part. V., Chapter 3 Shore Protection Projects, EM 1110-2-110. *Coastal and Hydraulics Lab., US Army Engineer Research and Development Center, Vicksburg, Mississippi, USA*.

U.S. Geological Survey (2012a). *2012 USGS EAARL-B Lidar: Post-Sandy (NJ)*. St. Petersburg Coastal and Marine Science Center. http://www.csc.noaa.gov/digitalcoast/data/coastallidar/download, Accessed 30 September 2014.

U.S. Geological Survey (2012b). *2012 USGS EAARL-B Lidar: Pre-Sandy (NJ)*. St. Petersburg Coastal and Marine Science Center. http://www.csc.noaa.gov/digitalcoast/data/coastallidar/download, Accessed 30 June 2014.

U.S. Geological Survey National Water Information System (2012). *USGS 01408168 Barnegat Bay at Mantoloking NJ*. U.S. Geological Survey. http://waterdata.usgs.gov/usa/nwis/uv?01408168, Accessed 14 January 2014.

Van Rijn, L., Walstra, D., Grasmeijer, B., Sutherland, J., Pan, S., and Sierra, J. (2003). The predictability of cross-shore bed evolution of sandy beaches at the time scale of storms and seasons using process-based profile models. *Coastal Engineering*, 47(3):295–327.

Van Thiel de Vries, J. S. M. (2009). *Dune erosion during storm surges*. PhD thesis, TU Delft, Delft University of Technology.

Van Thiel de Vries, J. S. M. (2012). Dune erosion above revetments. *ICCE 2012: Proceedings of the 33rd International Conference on Coastal Engineering, Santander, Spain, 1-6 July 2012*.

van Verseveld, H., van Dongeren, A., Plant, N., Jäger, W., and den Heijer, C. (2015). Modelling multi-hazard hurricane damages on an urbanized coast with a bayesian network approach. *Coastal Engineering*, 103:1–14.

Williams, A. M., Feagin, R. A., Smith, W. K., and Jackson, N. L. (2009). Ecosystem impacts of Hurricane Ike on Galveston Island and Bolivar Peninsula: perspectives of the coastal barrier island network (CBIN). *Shore & Beach*, 77(2):71.

Williams, S. J. (2013). Sea-level rise implications for coastal regions. *Journal of Coastal Research*, 63(sp1):184–196.

Woodruff, J. D., Irish, J. L., and Camargo, S. J. (2013). Coastal flooding by tropical cyclones and sea-level rise. *Nature*, 504(7478):44–52.

Wright, C. W., Troche, R. J., Klipp, E. S., Kranenburg, C. J., Fredericks, A. M., and Nagle, D. B. (2014). EAARL-B submerged topography: Barnegat Bay, New Jersey, pre-Hurricane Sandy, 2012. Technical Report Data Series 885, U.S. Geological Survey. http://pubs.er.usgs.gov/publication/ds885, Accessed 14 November 2014.

XBeach Technical Reference (2015). *XBeach Technical Reference: Kingsday Release*. Deltares. http://oss.deltares.nl/documents/48999/49476/XBeach_manual_Kingsday.pdf.

Yang, B., Hwang, C., and Cordell, H. K. (2012). Use of lidar shoreline extraction for analyzing revetment rock beach protection: A case study of Jekyll Island State Park, USA. *Ocean & Coastal Management*, 69:1–15.

Yang, R.-Y., Wu, Y.-C., Hwung, H.-H., Liou, J.-Y., and Shugan, I. V. (2010). Current countermeasure of beach erosion control and its application in Taiwan. *Ocean & Coastal Management*, 53(9):552–561.

Yin, J., Schlesinger, M. E., and Stouffer, R. J. (2009). Model projections of rapid sea-level rise on the northeast coast of the United States. *Nature Geoscience*, 2(4):262–266.

Appendix A

XBeach

XBeach is a two-dimensional horizontal (2DH) finite difference model originally developed to simulate hydrodynamics and morphology on sandy coasts in response to time-varying storm conditions (Roelvink et al., 2009; XBeach Technical Reference, 2015). According to the impact regimes defined by Sallenger (2000), XBeach accurately simulates infragravity swash, dune erosion, overwash and inundation of barrier islands (McCall et al., 2010; Roelvink et al., 2009).

To simulate these processes, the wave-group resolving model solves model equations using an upwind explicit scheme with automatic time step, such that wave conditions and water levels are imposed as offshore boundary conditions. A staggered grid is applied such that water levels, bed levels, and concentrations (e.g. sediment concentrations) are determined at cell centers and velocities and sediment transport are determined at cell interfaces. Four main modules comprise XBeach, and these are described below.

Wave boundary conditions are input into the short wave module to solve a wave action balance equation given by

$$\frac{\partial A}{\partial t} + \frac{\partial c_{gx} A}{\partial x} + \frac{\partial c_{gy} A}{\partial y} + \frac{\partial c_{\theta} A}{\partial \theta} = -\frac{D_w}{\sigma} \tag{A.1}$$

where A is wave action, c_g is group velocity, θ is angle of incidence, D_w is wave energy dissipation and σ is wave frequency. D_w acts as a source term in the roller energy balance, which is coupled with Equation (A.1) to account for the shoreward shift of forcing due to energy stored in surface rollers.

Using radiation stress gradients from the wave module, the flow module solves the depth-averaged Generalized Lagrangian Mean equations:

$$\frac{\partial u^L}{\partial t} + u^L \frac{\partial u^L}{\partial x} + v^L \frac{\partial u^L}{\partial y} - f v^L - v_h \left(\frac{\partial^2 u^L}{\partial x^2} + \frac{\partial^2 u^L}{\partial y^2} \right) = -\frac{\tau_{bx}^E}{\rho h} - g \frac{\partial \eta}{\partial x} + \frac{F_x}{\rho h} \tag{A.2}$$

$$\frac{\partial v^L}{\partial t} + u^L \frac{\partial v^L}{\partial x} + v^L \frac{\partial v^L}{\partial y} + f u^L - v_h \left(\frac{\partial^2 v^L}{\partial x^2} + \frac{\partial^2 v^L}{\partial y^2} \right) = -\frac{\tau_{by}^E}{\rho h} - g \frac{\partial \eta}{\partial y} + \frac{F_y}{\rho h} \tag{A.3}$$

$$\frac{\partial \eta}{\partial t} + \frac{\partial h u^L}{\partial x} + \frac{\partial h v^L}{\partial y} = 0 \tag{A.4}$$

where u^L and v^L are Lagrangian velocities, τ_b^E is bed shear stress, F is wave-induced stress, f is a Coriolis coefficient, v_h is horizontal viscosity and η is water level. Linear wave theory is used to calculate radiation stress gradients, which are used to determine F in x and y directions.

Outputs from the wave and flow modules are then used in the sediment transport module to calculate sediment transport gradients. Sediment transport is determined using a depth-averaged advection-diffusion equation given by

$$\frac{\partial hC}{\partial t} + \frac{\partial hCu^E}{\partial x} + \frac{\partial hCv^E}{\partial y} + \frac{\partial}{\partial x}\left[D_h h \frac{\partial C}{\partial x} \right] + \frac{\partial}{\partial y}\left[D_h h \frac{\partial C}{\partial y} \right] = \frac{hC_{eq} - hC}{T_s} \tag{A.5}$$

where C is depth-averaged sediment concentration, D_h is a sediment diffusion coefficient, C_{eq} is equilibrium sediment concentration and T_s is the time of sediment entrainment. Small values of T_s causes an immediate sediment response, where sediment entrainment or deposition is dependent on the mismatch between C and C_{eq}.

The morphology module uses outputs from the flow and sediment transport modules to update bed levels. Bed level changes are based on the sediment transport gradients and storm-induced avalanching of the dune. At the beginning of the second time step, the updated bed levels are used in the short wave and flow modules to calculate hydrodynamics.

Full details about XBeach can be found in Roelvink et al. (2009) and XBeach Technical Reference (2015).

Appendix B

Data Management Plan

Due to the large volumes of data generated by each numerical simulation, raw data are not provided in this dissertation. On average, each simulation requires 1.75 GB of storage, which includes all input and output files. These data are available on a local machine (MacBook Pro, VT343695) and an external hard drive (Western Digital My Book, personally owned). Any data requests may be sent to Stephanie Smallegan: ssmalls@vt.edu.

Appendix C

License Agreement

The license agreement, obtained from Elsevier for reuse of the manuscript "Morphological response of a sandy barrier island with a buried seawall during Hurricane Sandy" presented in Chapter 2, is given below.

ELSEVIER LICENSE
TERMS AND CONDITIONS

Mar 25, 2016

This is a License Agreement between Stephanie M Smallegan ("You") and Elsevier ("Elsevier") provided by Copyright Clearance Center ("CCC"). The license consists of your order details, the terms and conditions provided by Elsevier, and the payment terms and conditions.

All payments must be made in full to CCC. For payment instructions, please see information listed at the bottom of this form.

Supplier	Elsevier Limited The Boulevard,Langford Lane Kidlington,Oxford,OX5 1GB,UK
Registered Company Number	1982084
Customer name	Stephanie M Smallegan
Customer address	150 Jaguar Dr. MOBILE, AL 36688
License number	3836061039372
License date	Mar 25, 2016
Licensed content publisher	Elsevier
Licensed content publication	Coastal Engineering
Licensed content title	Morphological response of a sandy barrier island with a buried seawall during Hurricane Sandy
Licensed content author	Stephanie M. Smallegan,Jennifer L. Irish,Ap R. Van Dongeren,Joost P. Den Bieman
Licensed content date	April 2016
Licensed content volume number	110
Licensed content issue number	n/a
Number of pages	9
Start Page	102
End Page	110
Type of Use	reuse in a thesis/dissertation
Portion	full article
Format	both print and electronic
Are you the author of this Elsevier article?	Yes
Will you be translating?	No
Title of your	Morphological change of a developed barrier island due to hurricane

thesis/dissertation	forcing
Expected completion date	Apr 2016
Estimated size (number of pages)	80
Elsevier VAT number	GB 494 6272 12
Permissions price	0.00 USD
VAT/Local Sales Tax	0.00 USD / 0.00 GBP
Total	0.00 USD

Terms and Conditions

INTRODUCTION

1. The publisher for this copyrighted material is Elsevier. By clicking "accept" in connection with completing this licensing transaction, you agree that the following terms and conditions apply to this transaction (along with the Billing and Payment terms and conditions established by Copyright Clearance Center, Inc. ("CCC"), at the time that you opened your Rightslink account and that are available at any time at http://myaccount.copyright.com).

GENERAL TERMS

2. Elsevier hereby grants you permission to reproduce the aforementioned material subject to the terms and conditions indicated.
3. Acknowledgement: If any part of the material to be used (for example, figures) has appeared in our publication with credit or acknowledgement to another source, permission must also be sought from that source. If such permission is not obtained then that material may not be included in your publication/copies. Suitable acknowledgement to the source must be made, either as a footnote or in a reference list at the end of your publication, as follows:
"Reprinted from Publication title, Vol /edition number, Author(s), Title of article / title of chapter, Pages No., Copyright (Year), with permission from Elsevier [OR APPLICABLE SOCIETY COPYRIGHT OWNER]." Also Lancet special credit - "Reprinted from The Lancet, Vol. number, Author(s), Title of article, Pages No., Copyright (Year), with permission from Elsevier."
4. Reproduction of this material is confined to the purpose and/or media for which permission is hereby given.
5. Altering/Modifying Material: Not Permitted. However figures and illustrations may be altered/adapted minimally to serve your work. Any other abbreviations, additions, deletions and/or any other alterations shall be made only with prior written authorization of Elsevier Ltd. (Please contact Elsevier at permissions@elsevier.com)
6. If the permission fee for the requested use of our material is waived in this instance, please be advised that your future requests for Elsevier materials may attract a fee.
7. Reservation of Rights: Publisher reserves all rights not specifically granted in the combination of (i) the license details provided by you and accepted in the course of this licensing transaction, (ii) these terms and conditions and (iii) CCC's Billing and Payment terms and conditions.
8. License Contingent Upon Payment: While you may exercise the rights licensed immediately upon issuance of the license at the end of the licensing process for the transaction, provided that you have disclosed complete and accurate details of your proposed use, no license is finally effective unless and until full payment is received from you (either by publisher or by CCC) as provided in CCC's Billing and Payment terms and conditions. If full payment is not received on a timely basis, then any license preliminarily granted shall be deemed automatically revoked and shall be void as if never granted. Further, in the event

that you breach any of these terms and conditions or any of CCC's Billing and Payment terms and conditions, the license is automatically revoked and shall be void as if never granted. Use of materials as described in a revoked license, as well as any use of the materials beyond the scope of an unrevoked license, may constitute copyright infringement and publisher reserves the right to take any and all action to protect its copyright in the materials.

9. Warranties: Publisher makes no representations or warranties with respect to the licensed material.

10. Indemnity: You hereby indemnify and agree to hold harmless publisher and CCC, and their respective officers, directors, employees and agents, from and against any and all claims arising out of your use of the licensed material other than as specifically authorized pursuant to this license.

11. No Transfer of License: This license is personal to you and may not be sublicensed, assigned, or transferred by you to any other person without publisher's written permission.

12. No Amendment Except in Writing: This license may not be amended except in a writing signed by both parties (or, in the case of publisher, by CCC on publisher's behalf).

13. Objection to Contrary Terms: Publisher hereby objects to any terms contained in any purchase order, acknowledgment, check endorsement or other writing prepared by you, which terms are inconsistent with these terms and conditions or CCC's Billing and Payment terms and conditions. These terms and conditions, together with CCC's Billing and Payment terms and conditions (which are incorporated herein), comprise the entire agreement between you and publisher (and CCC) concerning this licensing transaction. In the event of any conflict between your obligations established by these terms and conditions and those established by CCC's Billing and Payment terms and conditions, these terms and conditions shall control.

14. Revocation: Elsevier or Copyright Clearance Center may deny the permissions described in this License at their sole discretion, for any reason or no reason, with a full refund payable to you. Notice of such denial will be made using the contact information provided by you. Failure to receive such notice will not alter or invalidate the denial. In no event will Elsevier or Copyright Clearance Center be responsible or liable for any costs, expenses or damage incurred by you as a result of a denial of your permission request, other than a refund of the amount(s) paid by you to Elsevier and/or Copyright Clearance Center for denied permissions.

LIMITED LICENSE

The following terms and conditions apply only to specific license types:

15. **Translation**: This permission is granted for non-exclusive world **English** rights only unless your license was granted for translation rights. If you licensed translation rights you may only translate this content into the languages you requested. A professional translator must perform all translations and reproduce the content word for word preserving the integrity of the article.

16. **Posting licensed content on any Website**: The following terms and conditions apply as follows: Licensing material from an Elsevier journal: All content posted to the web site must maintain the copyright information line on the bottom of each image; A hyper-text must be included to the Homepage of the journal from which you are licensing at http://www.sciencedirect.com/science/journal/xxxxx or the Elsevier homepage for books at http://www.elsevier.com; Central Storage: This license does not include permission for a scanned version of the material to be stored in a central repository such as that provided by Heron/XanEdu.

Licensing material from an Elsevier book: A hyper-text link must be included to the Elsevier homepage at http://www.elsevier.com . All content posted to the web site must maintain the copyright information line on the bottom of each image.

Posting licensed content on Electronic reserve: In addition to the above the following clauses are applicable: The web site must be password-protected and made available only to bona fide students registered on a relevant course. This permission is granted for 1 year only. You may obtain a new license for future website posting.
17. **For journal authors:** the following clauses are applicable in addition to the above:
Preprints:
A preprint is an author's own write-up of research results and analysis, it has not been peer-reviewed, nor has it had any other value added to it by a publisher (such as formatting, copyright, technical enhancement etc.).
Authors can share their preprints anywhere at any time. Preprints should not be added to or enhanced in any way in order to appear more like, or to substitute for, the final versions of articles however authors can update their preprints on arXiv or RePEc with their Accepted Author Manuscript (see below).
If accepted for publication, we encourage authors to link from the preprint to their formal publication via its DOI. Millions of researchers have access to the formal publications on ScienceDirect, and so links will help users to find, access, cite and use the best available version. Please note that Cell Press, The Lancet and some society-owned have different preprint policies. Information on these policies is available on the journal homepage.
Accepted Author Manuscripts: An accepted author manuscript is the manuscript of an article that has been accepted for publication and which typically includes author-incorporated changes suggested during submission, peer review and editor-author communications.
Authors can share their accepted author manuscript:

- immediately
    - via their non-commercial person homepage or blog
    - by updating a preprint in arXiv or RePEc with the accepted manuscript
    - via their research institute or institutional repository for internal institutional uses or as part of an invitation-only research collaboration work-group
    - directly by providing copies to their students or to research collaborators for their personal use
    - for private scholarly sharing as part of an invitation-only work group on commercial sites with which Elsevier has an agreement
- after the embargo period
    - via non-commercial hosting platforms such as their institutional repository
    - via commercial sites with which Elsevier has an agreement

In all cases accepted manuscripts should:

- link to the formal publication via its DOI
- bear a CC-BY-NC-ND license - this is easy to do
- if aggregated with other manuscripts, for example in a repository or other site, be shared in alignment with our hosting policy not be added to or enhanced in any way to appear more like, or to substitute for, the published journal article.

Published journal article (JPA): A published journal article (PJA) is the definitive final record of published research that appears or will appear in the journal and embodies all value-adding publishing activities including peer review co-ordination, copy-editing, formatting, (if relevant) pagination and online enrichment.
Policies for sharing publishing journal articles differ for subscription and gold open access

articles:

Subscription Articles: If you are an author, please share a link to your article rather than the full-text. Millions of researchers have access to the formal publications on ScienceDirect, and so links will help your users to find, access, cite, and use the best available version.
Theses and dissertations which contain embedded PJAs as part of the formal submission can be posted publicly by the awarding institution with DOI links back to the formal publications on ScienceDirect.
If you are affiliated with a library that subscribes to ScienceDirect you have additional private sharing rights for others' research accessed under that agreement. This includes use for classroom teaching and internal training at the institution (including use in course packs and courseware programs), and inclusion of the article for grant funding purposes.
Gold Open Access Articles: May be shared according to the author-selected end-user license and should contain a CrossMark logo, the end user license, and a DOI link to the formal publication on ScienceDirect.
Please refer to Elsevier's posting policy for further information.
18. **For book authors** the following clauses are applicable in addition to the above:
Authors are permitted to place a brief summary of their work online only. You are not allowed to download and post the published electronic version of your chapter, nor may you scan the printed edition to create an electronic version. **Posting to a repository:** Authors are permitted to post a summary of their chapter only in their institution's repository.
19. **Thesis/Dissertation**: If your license is for use in a thesis/dissertation your thesis may be submitted to your institution in either print or electronic form. Should your thesis be published commercially, please reapply for permission. These requirements include permission for the Library and Archives of Canada to supply single copies, on demand, of the complete thesis and include permission for Proquest/UMI to supply single copies, on demand, of the complete thesis. Should your thesis be published commercially, please reapply for permission. Theses and dissertations which contain embedded PJAs as part of the formal submission can be posted publicly by the awarding institution with DOI links back to the formal publications on ScienceDirect.

Elsevier Open Access Terms and Conditions

You can publish open access with Elsevier in hundreds of open access journals or in nearly 2000 established subscription journals that support open access publishing. Permitted third party re-use of these open access articles is defined by the author's choice of Creative Commons user license. See our open access license policy for more information.
Terms & Conditions applicable to all Open Access articles published with Elsevier:
Any reuse of the article must not represent the author as endorsing the adaptation of the article nor should the article be modified in such a way as to damage the author's honour or reputation. If any changes have been made, such changes must be clearly indicated.
The author(s) must be appropriately credited and we ask that you include the end user license and a DOI link to the formal publication on ScienceDirect.
If any part of the material to be used (for example, figures) has appeared in our publication with credit or acknowledgement to another source it is the responsibility of the user to ensure their reuse complies with the terms and conditions determined by the rights holder.
Additional Terms & Conditions applicable to each Creative Commons user license:
CC BY: The CC-BY license allows users to copy, to create extracts, abstracts and new works from the Article, to alter and revise the Article and to make commercial use of the Article (including reuse and/or resale of the Article by commercial entities), provided the user gives appropriate credit (with a link to the formal publication through the relevant DOI), provides a link to the license, indicates if changes were made and the licensor is not represented as endorsing the use made of the work. The full details of the license are

available at http://creativecommons.org/licenses/by/4.0.
CC BY NC SA: The CC BY-NC-SA license allows users to copy, to create extracts, abstracts and new works from the Article, to alter and revise the Article, provided this is not done for commercial purposes, and that the user gives appropriate credit (with a link to the formal publication through the relevant DOI), provides a link to the license, indicates if changes were made and the licensor is not represented as endorsing the use made of the work. Further, any new works must be made available on the same conditions. The full details of the license are available at http://creativecommons.org/licenses/by-nc-sa/4.0.
CC BY NC ND: The CC BY-NC-ND license allows users to copy and distribute the Article, provided this is not done for commercial purposes and further does not permit distribution of the Article if it is changed or edited in any way, and provided the user gives appropriate credit (with a link to the formal publication through the relevant DOI), provides a link to the license, and that the licensor is not represented as endorsing the use made of the work. The full details of the license are available at http://creativecommons.org/licenses/by-nc-nd/4.0.
Any commercial reuse of Open Access articles published with a CC BY NC SA or CC BY NC ND license requires permission from Elsevier and will be subject to a fee.
Commercial reuse includes:

- Associating advertising with the full text of the Article
- Charging fees for document delivery or access
- Article aggregation
- Systematic distribution via e-mail lists or share buttons

Posting or linking by commercial companies for use by customers of those companies.

20. **Other Conditions**:

v1.8